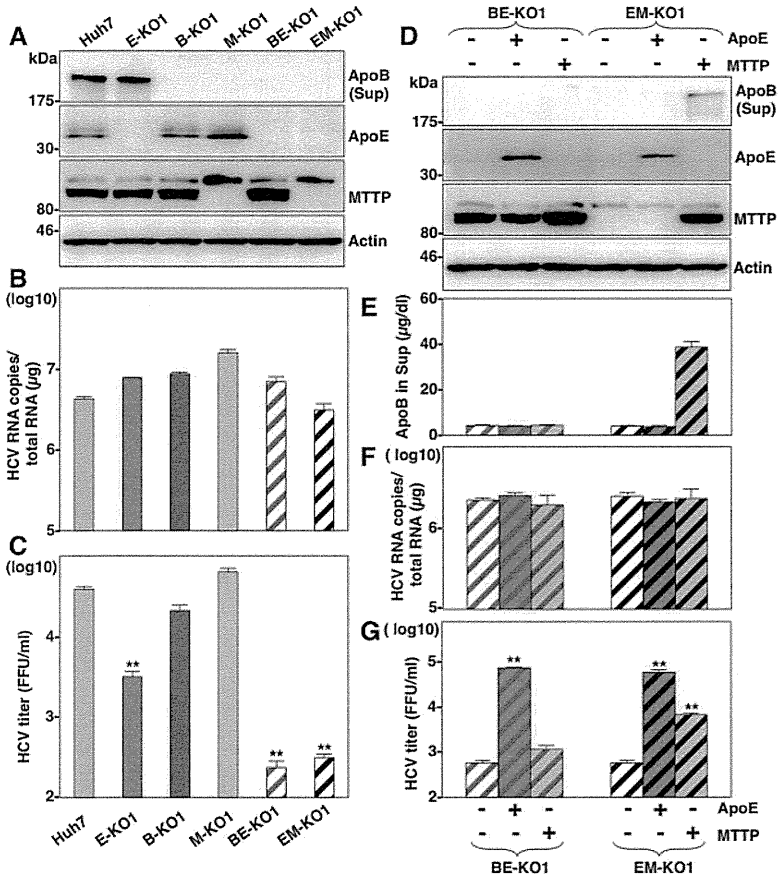

Figure 3. MTTP participates in the formation of infectious HCV particles through the maturation of ApoB. (A) Expressions of ApoB, ApoE and MTTP in Huh7, B-KO1, M-KO1, E-KO1, BE-KO1 and EM-KO1 cells were determined by immunoblotting analysis. Cells were infected with HCVcc at an MOI of 1, and intracellular HCV RNA (B) and infectious titers in the supernatants (C) were determined at 72 h post-infection by qRT-PCR and focus-forming assay, respectively. The expressions of ApoB, ApoE and MTTP in BE-KO1 and EM-KO1 cells with/without expression of ApoE or MTTP by lentiviral vector were determined by immunoblotting (D) and ELISA (E). Cells were infected with HCVcc at an MOI of 1, and intracellular HCV RNA (F) and infectious titers in the supernatants (G) were determined at 72 h post-infection by qRT-PCR and focus-forming assay, respectively.
doi:10.1371/journal.ppat.1004534.g003

HCV particles in 293T-CLDN/miR-122 cells (Fig. 4E). On the other hand, the expression of ApoE exhibited no effect on the propagation of Japanese encephalitis virus (JEV) and dengue virus (DENV) (Figure S7) in BE-KO1 cells. These results suggest that the exchangeable apolipoproteins and ApoB redundantly and specifically participate in the formation of HCV particles.

To examine the role of exchangeable apolipoproteins in the formation of other genotypes of HCV, the effect of exogenous expression of these apolipoproteins on the propagation of genotype 1b and 3a chimeric HCVcc, TH/JFH1 and S310/JFH1 viruses in BE-KO1 cells was determined (Fig. 5) [22,23]. As seen in infection with HCVcc (JFH1), expression of ApoA1, ApoA2, ApoC1, ApoC2, ApoC3 and ApoE enhanced the formation of infectious particles of TH/JFH1 and S310/JFH1 chimeric viruses. These results suggest that ApoA1, ApoA2, ApoC1, ApoC2, ApoC3 and ApoE redundantly participate in the efficient formation of infectious HCV particles of genotypes 1b, 2a and 3a.

Apolipoproteins participate in the post-envelopment step of particle formation

To determine the details of the assembly of infectious HCV particles in the BE-KO1 cells, intracellular infectious titers were determined in Huh7, BE-KO1 and ApoE-res cells by using the freeze and thaw method. Not only intracellular but also extracellular infection titers were impaired in BE-KO1 cells compared with those in parental and ApoE-res cells (Fig. 6A), suggesting that intracellular particle formation is impaired by deficiencies in the expression of ApoB and ApoE. Previous reports have shown that the recruitment of viral proteins around LD and redistribution of LD are essential for HCV assembly [24]. To clarify the roles of the exchangeable apolipoproteins on HCV assembly in more detail, we examined the intracellular localization of viral proteins, LD and ER in BE-KO1 and ApoE-res cells. The localization of core proteins around LD and the membranous-web structure forming the replication complex were observed in BE-KO1 cells upon infection with HCVcc, as reported in parental Huh7 cells (Fig. 6B, 6C and Figure S8). However, greater accumulation of core proteins and LD around the perinuclear region was detected in BE-KO1 cells in comparison with ApoE-res cells (Fig. 6C and 6D), supporting the notion that apolipoproteins participate in the infectious particle formation in HCV rather than viral RNA replication. Previous studies revealed that core proteins were mainly localized on the ER membrane upon infection with the genotype 2a Jc1 strain-based HCVcc (HCVcc/Jc1), and inhibition of capsid assembly and envelopment caused accumulation of core proteins on the surface of LD [25–27]. In ApoE-res cells, core proteins of HCVcc/Jc1 were mainly localized on the

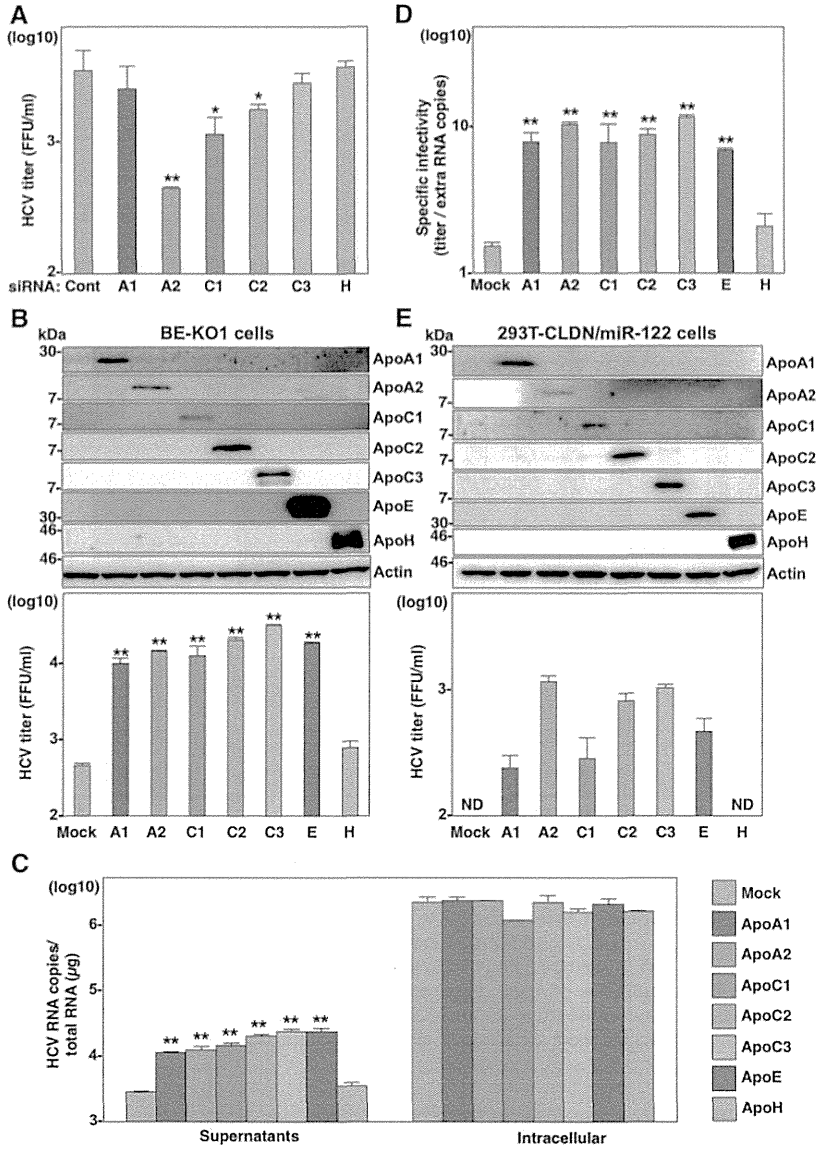

Figure 4. Exchangeable apolipoproteins redundantly participate in the formation of infectious HCV particles. (A) BE-KO1 cells infected with HCVcc at an MOI of 1 at 6 h post-transfection with siRNAs targeting ApoA1 (A1), ApoA2 (A2), ApoC1 (C1), ApoC2 (C2), ApoC3 (C3) and ApoH (H) and infectious titers in the culture supernatants were determined by focus-forming assay at 72 h post-infection. (B) ApoA1, ApoA2, ApoC1, ApoC2, ApoC3, ApoE and ApoH were exogenously expressed in BE-KO1 cells by infection with lentiviral vectors, and then infected with HCVcc at an MOI of 1. Expression of the apolipoproteins was determined by immunoblot analysis (upper), and infectious titers in the culture supernatants were determined at 72 h post-infection by focus-forming assay (lower). (C) Extracellular and intracellular HCV RNA in BE-KO1 cells expressing apolipoproteins and infected with HCVcc were determined at 72 h post-infection by qRT-PCR. (D) Specific infectivity was calculated as extracellular infectious titers/ extracellular HCV RNA copies in BE-KO1 cells expressing apolipoproteins at 72 h post-infection. (E) 293T cells stably expressing CLDN1 and miR-122 (293T-CLDN/miR-122 cells) were infected with the lentiviral vectors, and the expressions of the apolipoproteins were determined by immunoblot analysis (upper). These cells were infected with HCVcc at an MOI of 1, and infectious titers in the supernatants were determined at 72 h post-infection by focus-forming assay (lower). In all cases, asterisks indicate significant differences (*, $P<0.05$; **, $P<0.01$) versus the results for control cells.
doi:10.1371/journal.ppat.1004534.g004

ER membrane, in contrast to the co-localization of core proteins of HCVcc (JFH1) with LD (Fig. 6E upper). However, core proteins were accumulated around LD in BE-KO1 cells infected with HCVcc/Jc1, as seen in those infected with HCVcc (JFH1) (Fig. 6E lower). These results suggest that apolipoproteins participate in the steps of HCV particle formation occurring after HCV protein assembly on the LD.

To further examine the involvement of apolipoproteins in the infectious particle formation of HCV, culture supernatants and cell lysates of BE-KO1 and ApoE-res cells infected with HCVcc were analyzed by buoyant density ultracentrifugation (Fig. 7A–B) [28]. Secretion of viral capsids in the supernatants was severely impaired in BE-KO1 cells in comparison with that in ApoE-res cells (Fig. 7A upper), in contrast to the detection of abundant intracellular capsids in both cell lines (Fig. 7B upper). Although peak levels of the core proteins and infectious titers were detected around 1.08 g/ml in both cell lines, the infectious titers in all fractions of BE-KO1 cells were significantly lower than those in ApoE-res cells, supporting the notion that apolipoproteins participate in the post-assembly process of HCV capsids which

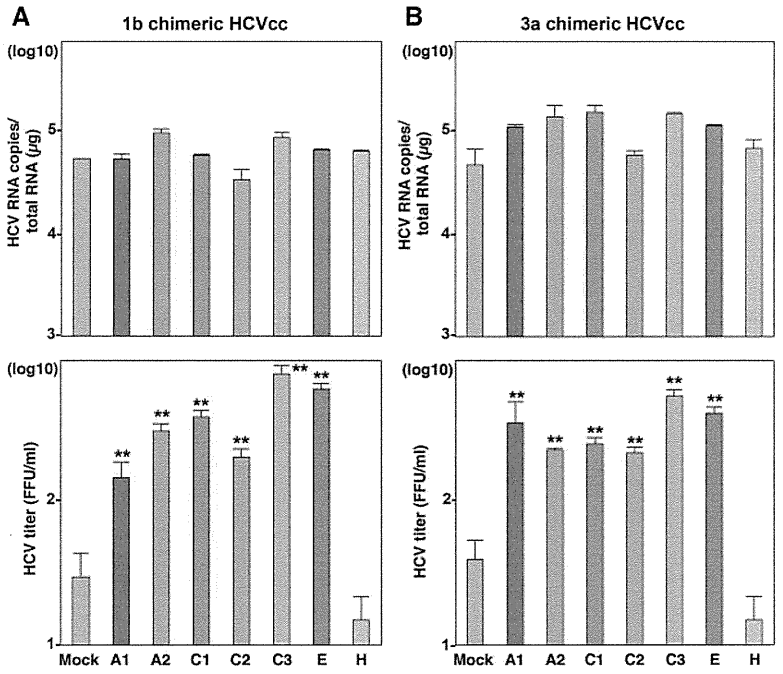

Figure 5. Exchangeable apolipoproteins participate in the formation of infectious HCV particles of genotype 1 and 3. ApoA1, ApoA2, ApoC1, ApoC2, ApoC3, ApoE and ApoH were exogenously expressed in BE-KO1 cells by infection with lentiviral vectors, and then infected with genotype 1b and 3a chimeric HCVcc, TH/JFH1 (A) and S310/JFH1 (B) at an MOI of 0.5. Intracellular HCV RNA and infectious titers in the culture supernatants were determined at 72 h post-infection by qRT-PCR (upper) and focus-forming assay (lower). Asterisks indicate significant differences (**, $P<0.01$) versus the results for control cells.
doi:10.1371/journal.ppat.1004534.g005

is required to confer infectivity. Next, to examine the involvement of apolipoproteins in the envelopment of HCV particles, lysates of BE-KO1 and ApoE-res cells infected with HCVcc were treated with proteinase K in the presence or absence of Triton X [26]. Protection of HCV core proteins from the protease digestion was observed in both cell lysates (Fig. 7C), suggesting that apolipoproteins are not involved in the envelopment of HCV particles. Collectively, these results suggest that exchangeable apolipoproteins participate in the post-envelopment step of HCV particle formation.

Amphipathic α-helices in exchangeable apolipoproteins participate in the formation of infectious HCV particles through the interaction with viral particles

To determine the structural relevance of apolipoproteins involved in the HCV assembly, the secondary structures of the apolipoproteins were deduced by using a CLC Genomics Workbench and previous reports (Fig. 8A) [29–34]. Tandem repeats of amphipathic α-helices were observed in the apolipoproteins capable of rescuing HCV assembly in BE-KO1 cells, but not in those lacking this activity, suggesting that amphipathic α-helices in the apolipoproteins participate in the assembly of HCV. To examine the involvement of the amphipathic α-helices of the exchangeable apolipoproteins in the particle formation of HCV, we constructed expression plasmids encoding deletion mutants of ApoE and ApoC1, and then these deletion mutants were exogenously expressed in BE-KO1 cells by lentiviral vectors (Fig. 8B and C upper panels). The expression of all of the deletion mutants of ApoE and ApoC1 containing either N-terminal or C-terminal amphipathic α-helices rescued the particle formation of HCV in BE-KO1 cells (Fig. 8B and C lower panels), suggesting that amphipathic α-helices in the apolipoproteins play crucial roles in the production of infectious HCV particles. In addition, more abundant full-length and truncated ApoE were detected in the precipitates of the culture supernatants of cells infected with HCVcc than those of mock-infected cells concentrated by ultracentrifugation, suggesting that the amphipathic α-helices of apolipoproteins are directly associated with HCV particles (Fig. 8D and E). Taken together, the data in this study strongly suggest that exchangeable apolipoproteins redundantly participate in the infectious particle formation of HCV through the interaction between amphipathic α-helices and viral particles.

Discussion

In this study, we demonstrated the redundant roles of ApoB and the exchangeable apolipoproteins ApoA1, ApoA2, ApoC1, ApoC2, ApoC3 and ApoE in the assembly of infectious HCV particles. The deficiencies of both ApoB and ApoE inhibited the production of infectious HCV particles in Huh7 cells, and exogenous expression of exchangeable apolipoproteins rescued the particle formation. cDNA microarray revealed that the expression patterns of exchangeable apolipoproteins in hepatic cancer cell lines are widely different from those in liver tissue. In previous reports, ApoE and ApoB were identified as important host factors for the assembly of infectious HCV particles [10,11], and knockdown of ApoE and ApoB expression also inhibited the production of infectious particles in this study. Because ApoB and ApoE are major apolipoproteins in VLDL, several reports have suggested that the VLDL production machinery participates in the production of HCV particles. Furthermore, density gradient analyses revealed co-fractionation of HCV RNA with lipoproteins, with the resulting complexes being termed lipoviroparticles (LVP) [12,35]. However, it has been reported that there is no correlation between secretion of VLDL and production of LVP [36]. In

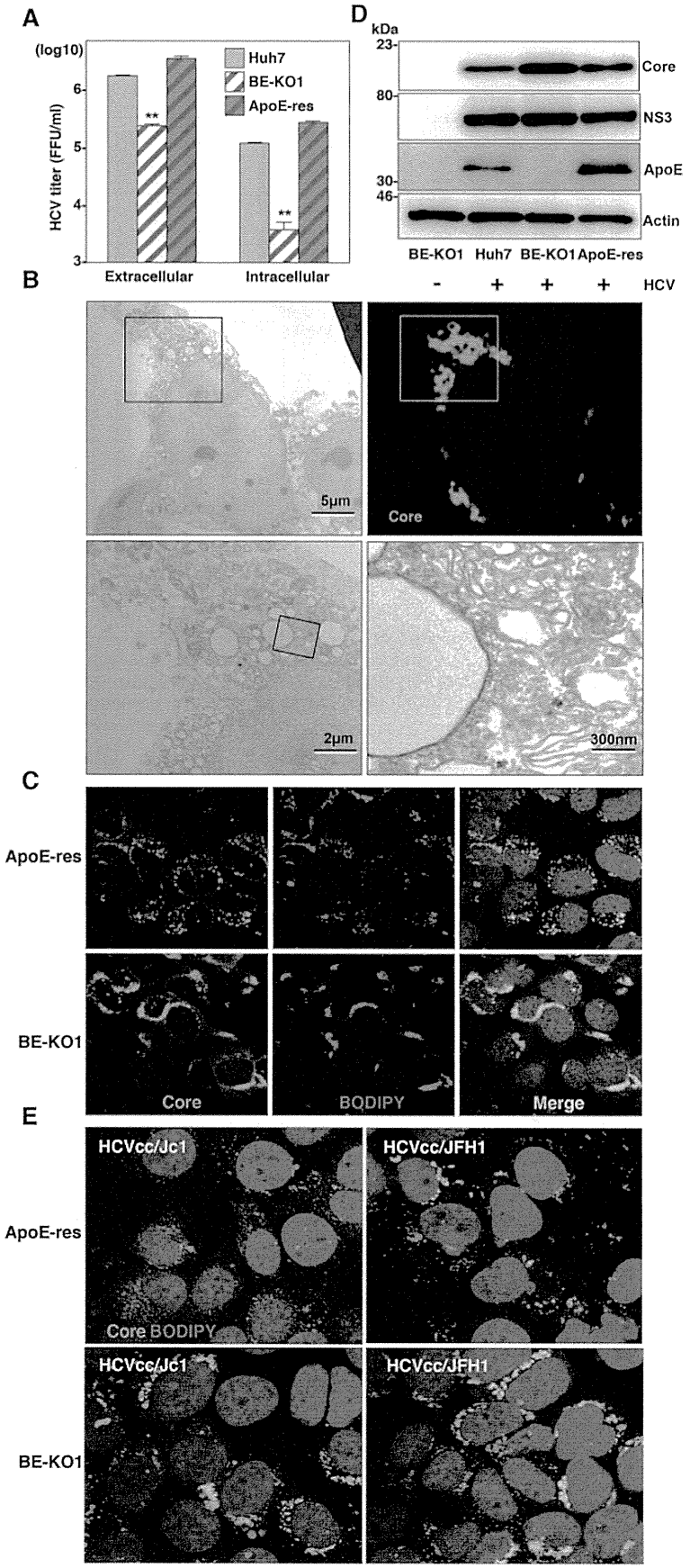
A
(log10)
HCV titer (FFU/ml)
Huh7
BE-KO1
ApoE-res
Extracellular
Intracellular
D
kDa
Core
NS3
ApoE
Actin
BE-KO1 Huh7 BE-KO1 ApoE-res
HCV
B
5μm
Core
2μm
300nm
C
ApoE-res
BE-KO1
Core
BODIPY
Merge
E
HCVcc/Jc1
HCVcc/JFH1
ApoE-res
Core BODIPY
BE-KO1

Figure 6. Accumulation of core proteins around lipid droplets in BE-KO1 cells. (A) Extracellular and intracellular infectious titers in Huh7, BE-KO1 and ApoE-restored cells infected by lentiviral vector (ApoE-res) were determined at 72 h post-infection with HCVcc at an MOI of 1 by focus-forming assay. Asterisks indicate significant differences (**, $P<0.01$) versus the results for parental cells. (B) BE-KO1 cells infected with HCVcc at an MOI of 1 were stained with anti-Core antibody at 72 h post-infection and examined by fluorescence microscopy. Identical fields were observed under electron microscopy by using the correlative FM-EM technique. The boxed areas are magnified and displayed. Huh7, BE-KO1 and ApoE-res cells infected with HCVcc at an MOI of 1 were subjected to immunofluorescence analyses by using anti-Core antibody (C), and immunoblotting by using antibodies against Core, NS3, ApoE, and actin at 72 h post-infection (D). Lipid droplets and cell nuclei were stained by BODIPY and DAPI, respectively. (E) BE-KO1 and ApoE-res cells infected with Jc1 strain-based HCVcc (HCVcc/Jc1; left panel) or JFH1 strain-based HCVcc (HCVcc/JFH1; right panel) at an MOI of 1 were subjected to immunofluorescence analysis by using anti-Core antibody at 72 h post-infection. Lipid droplets and cell nuclei were stained by BODIPY and DAPI, respectively.
doi:10.1371/journal.ppat.1004534.g006

addition, exogenous expression of ApoE facilitated the infectious particle formation of HCV in 293T cells stably expressing CLDN1 and miR-122 [16], suggesting that ApoE-mediated particle formation is independent from VLDL production. Furthermore, exogenous expression of ApoA1, a major apolipoprotein of HDL, also facilitated the production of HCV particles as shown in Fig. 4E. These data suggest that the roles of the exchangeable apolipoproteins in HCV assembly are independent from the production of VLDL. MTTP plays crucial roles in the lipoprotein formation through the incorporation of triglyceride into growing lipoprotein and secretion of ApoB [21]. Although it has been shown that treatment with an MTTP inhibitor impairs the production of HCV particles [11], in this study, we found that knockout of MTTP abrogated the secretion of ApoB but not the production of infectious HCV particles. Collectively, these data suggest that exchangeable apolipoproteins redundantly participate in the infectious particle formation of HCV independently from lipoprotein secretion machinery.

Production of HCV capsids in the culture supernatants is impaired in 293T cells expressing miR-122 due to lack of ApoE expression, but envelopment of viral capsids is observed [37], suggesting that ApoE is involved in the post-envelopment step. Coller et al. suggested that ApoE is associated with *de novo* formation of HCV particles during secretory pathway based on an experiment using HCV possessing a tetracysteine-tag in the core protein [38]. In this study, ApoA1, ApoA2, ApoC1, ApoC2, ApoC3 and ApoE enhanced the formation of HCV particles in the post-envelopment step. These results suggest that a direct interaction between exchangeable apolipoproteins and enveloped particles in the ER lumen facilitates an efficient secretion of infectious HCV particles. Ultrastructural analysis of HCV particles has shown that large amounts of apolipoproteins, including ApoA1, ApoB and ApoE, bind to the surface of viral particles [39]. Interestingly, ApoE-specific antibodies were more efficient in capturing viral particles than α-E1/E2 antibodies, and significantly large numbers of gold particles reacting with ApoE were observed per virion than those with E2, suggesting that viral envelope proteins are masked by a large amount of apolipoproteins. The unique characteristics of interaction between apolipoproteins and HCV particles might be applied for visualization of entry and purification of HCV particles by using GFP- or affinity-tagged amphipathic α-helices of apolipoproteins. In the previous report, virocidal amphipathic helical peptides impaired the infectivity of viral particles [40]. There is a possibility that such peptide influences on the interaction between apolipoproteins and viral particles, and might be a new therapeutic approach.

In previous reports, the importance of the interaction between lipoprotein receptors and ApoE in the entry of HCV has been well established. Lipoprotein receptors including scavenger receptor class B type 1 (SR-B1) and low-density lipoprotein receptor (LDLR) are involved in HCV entry into the target cells [41,42]. LDLR is thought to mediate cell attachment of HCV through an interaction with virus associated ApoE [43,44]. SR-B1 also interacts with ApoE and hypervariable region 1 (HVR1) in the envelope protein of HCV [43]. In this study we have shown that exchangeable apolipoproteins including not only ApoE but also ApoA and ApoC facilitate the production of infectious HCV particles, and that exchangeable apolipoproteins directly associate with viral particles. Meunier et al. reported that ApoC1 associates intracellularly with viral particles during particle morphogenesis and enhances the entry of HCV through an interaction of the C-terminal region of ApoC1 with heparan sulfate [45]. Another group also showed that ApoC1 enhances HCV infection through the triple interplay among HVR1, ApoC1, and SR-B1 [46]. These results suggest that the interaction of HCV particles with apolipoproteins also participates in the entry through the binding of lipoprotein receptors including SR-B1 and LDLR.

Although the gene-knockout technique is essential to obtain reproducible and reliable data, and many knockout mice have been produced in various research areas, the development of experimental tools for HCV study has also been hampered by the narrow cell tropism [47,48]. A humanized mouse model in which human liver cells were xenotransplanted into immunodeficient mouse was developed and provided an important platform for the analysis of pathogenesis and the development of antivirals for HCV [49]. However, the exogenous expression of human receptor molecules required for HCV entry and impairment of innate immunity are required for the complete propagation of HCV in mice [50]. Gene-knockout techniques using a CRISPR/Cas9 system composed of guide RNA and Cas9 nuclease that form RNA-protein complexes to cleave the target sequences [19] have allowed quick and easy establishment of gene-knockout mice and cancer cell lines [51,52], and indeed, such MTTP-knockout cell lines were established also in this study. Recently, the high-throughput screening of host factors involved in several conditions was reported by using a CRISPR/Cas9 system [53]. Together, these novel genome-editing techniques are expected to reveal the precise roles of host factors involved in the HCV life cycle.

In summary, we have shown that apolipoproteins, including ApoA1, ApoA2, ApoC1, ApoC2, ApoC3, ApoE and ApoB, possess redundant roles in the assembly of HCV through the interaction of the amphipathic α-helices in the apolipoproteins with viral particles in the post-envelopment step. It is hoped that these findings will provide clues to the life cycle of HCV and assist in the development of novel antivirals targeting the assembly process of HCV.

Materials and Methods

NextBio Body Atlas

The NextBio Body Atlas application presents an aggregated analysis of gene expression across various normal tissues, normal cell types, and cancer cell lines [20]. It enables us to investigate the expression of individual genes as well as gene sets. Samples for Body Atlas data are obtained from publicly available studies that are internally curated, annotated, and processed. Body Atlas

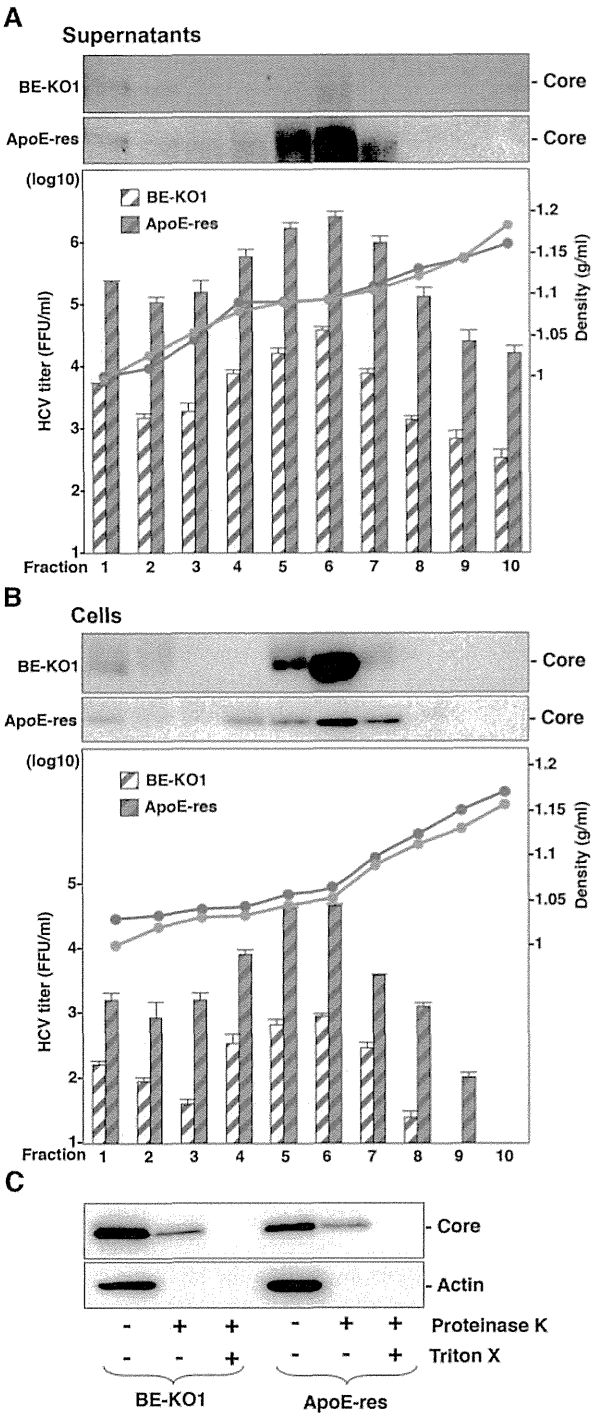

Figure 7. Apolipoproteins participate in the post-envelopment step of the HCV life cycle. The supernatants (A) and lysates (B) of BE-KO1 and ApoE-restored (ApoE-res) cells infected with HCVcc at an MOI of 1 were subjected to density gradient fractionation. Each fraction was subjected to immunoblotting using anti-Core antibody (upper). The infectious titers and densities of each fraction were determined (lower). (C) The lysates of BE-KO1 and ApoE-res cells infected with HCVcc at an MOI of 1 were subjected to proteinase K digestion protection assay. Lysates were separated into 3 parts and incubated for 1 h on ice in the presence or absence of 50 μg/ml proteinase K with/without pretreatment with 5% Triton-X and then subjected to immunoblotting.
doi:10.1371/journal.ppat.1004534.g007

measurements are generated from all available RNA expression studies that used Affymetrix U133 Plus or U133A Genechip Arrays for human studies. The results from 128 human tissue samples were incorporated from 1,067 arrays; 157 human cell types from 1,474 arrays; and 359 human cancer cell lines from 376 arrays. Gene queries return a list of relevant tissues or cell types rank-ordered by absolute gene expression and grouped by body systems or across all body systems. In the current analysis, we determined the expression levels of the apolipoproteins ApoA1, ApoA2, ApoB, ApoC1, ApoC2, ApoC3, ApoD, ApoE, ApoH, ApoL1, ApoL2 and ApoO in liver tissue. We used an analysis protocol developed by NextBio, the details of which have been described previously [20].

cDNA microarray

Expression profiling was generated using the 4 x 44 K whole human genome oligo-microarray ver.2.0 G4845A (Agilent Technologies) as previously described [54]. Raw data were imported into Subio platform ver.1.12 (Subio) for database management and quality control. Raw intensity data were normalized against GAPDH expression levels for further analysis. These raw data have been accepted by GEO (a public repository for microarray data, aimed at storing MIAME). Access to data concerning this study may be found under GEO experiment accession number GSE32886.

Cell lines

All cell lines were cultured at 37°C under the conditions of a humidified atmosphere and 5% CO_2. The human hepatocellular carcinoma-derived Huh7 and human embryonic kidney-derived 293T cells were obtained from Japanese Collection of Research Bioresources (JCRB) Cell Bank (JCRB0403 and JCRB9068), and maintained in DMEM (Sigma) supplemented with 100 U/ml penicillin, 100 μg/ml streptomycin, and 10% fetal calf serum (FCS). The Huh7-derived cell line Huh7.5.1 was kindly provided by F. Chisari. Huh7 cells harboring JFH1-based HCV-SGR were prepared according to the method of a previous report [54] and maintained in DMEM containing 10% FCS and 1 mg/ml G418 (Nakalai Tesque).

Plasmids

The cDNA clones of pri-miR-122, ApoA1, ApoA2, ApoC1, ApoC2, ApoC3, ApoE, ApoH, and AcGFP were inserted between the XhoI and XbaI sites of lentiviral vector pCSII-EF-RfA, which was kindly provided by M. Hijikata, and the resulting plasmids were designated pCSII-EF-miR-122, pCSII-EF-MT-apolipoproteins, and pCSII-EF-AcGFP, respectively. The deletion mutants of ApoC1 and ApoE were amplified by PCR and introduced into pCSII-EF. pHH-JFH1-E2p7NS2mt contains three adaptive mutations in pHH-JFH1 [55]. The pFL-J6/JFH1 plasmid that encodes the entire viral genome of the chimeric strain of HCV-2a, J6/JFH1, was kindly provided by Charles M. Rice [8]. pTH/JFH1 (genotype 1b) and pS310/JFH1 (genotype 3a) were used for the production of chimeric viruses [22,23]. The plasmid pX330, which encodes hCas9 and sgRNA, was obtained from Addgene (Addgene plasmid 42230). The fragments of guided RNA targeting the MTTP gene were inserted into the BbsI site of pX330 and designated pX330-MTTP. The plasmids used in this study were confirmed by sequencing with an ABI 3130 genetic analyzer (Life Technologies).

Antibodies

Mouse monoclonal antibodies to HCV core, β-actin and Calnexin were purchased from Thermo Scientific and Sigma Aldrich, respectively. Mouse anti-ApoA1, ApoB, ApoC1, ApoE

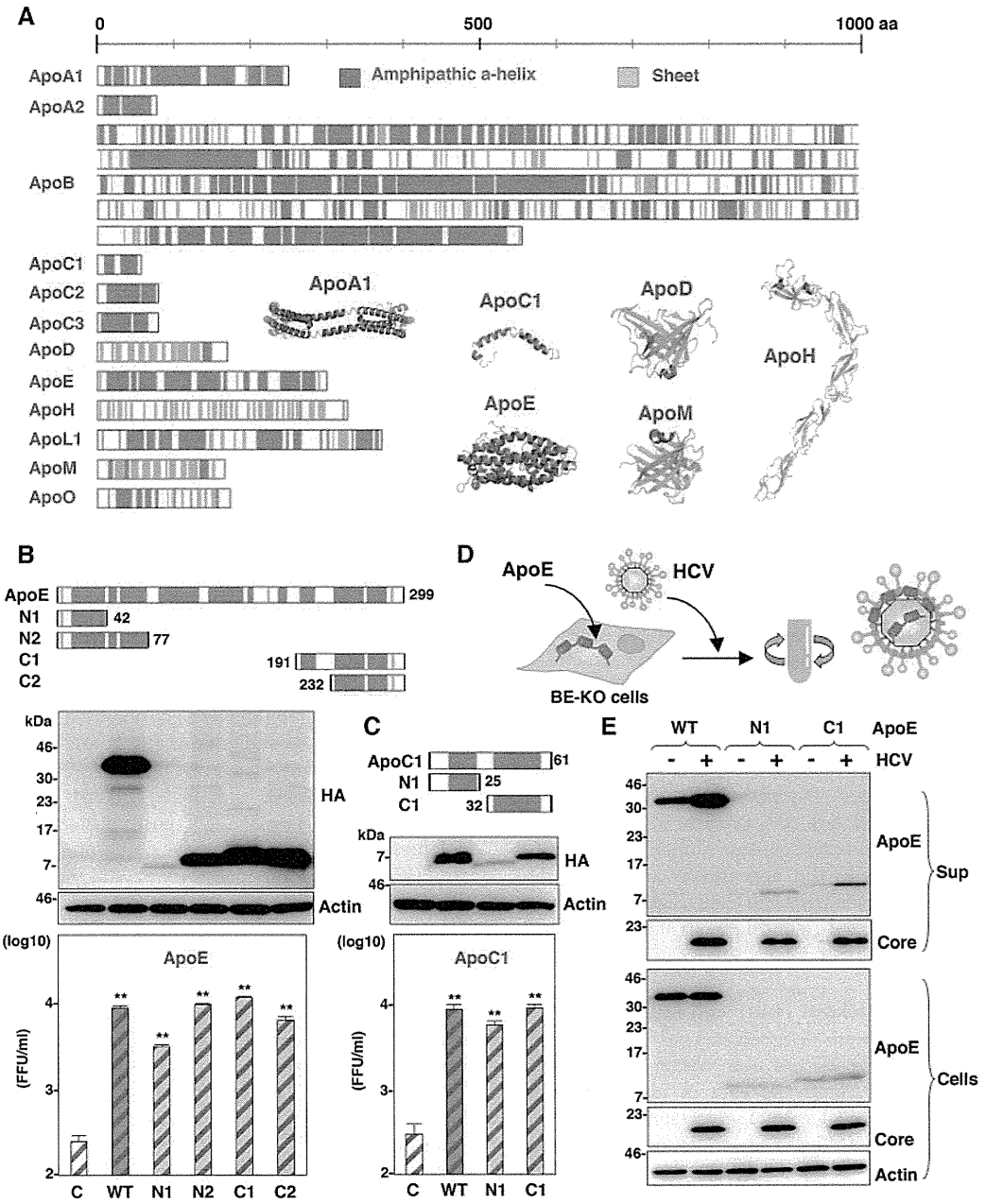

Figure 8. Amphipathic α-helices in apolipoproteins participate in the infectious particle formation of HCV. (A) Predicted or experimentally determined secondary structures of apolipoproteins. Secondary structures of the helices and sheets in the apolipoproteins are colored red and cyan, respectively. The three-dimensional structures of ApoA1 (Protein Data Bank (PDB) ID, 3R2P), ApoC1 (PDB ID, 1IOJ), ApoD (PDB ID, 2HZR), ApoE (PDB ID, 2L7B), ApoH (PDB ID, 1C1Z) and ApoM (PDB ID, 2XKL) are also shown in a ribbon model using the same color code of secondary structures. In cases in which the structure was not available, the secondary structure was predicted by using a CLC Genomics Workbench. (B,C) Schematics of the ApoE- and ApoC1-deletion mutants (upper). Deletion mutants with HA tags expressed in BE-KO1 cells by lentiviral vectors were detected by immunoblotting (middle). BE-KO1 cells expressing the WT or deletion mutants of ApoE or ApoC1 were infected with HCVcc at an MOI of 1, and infectious titers in the culture supernatants were determined by focus-forming assay at 72 h post-infection. Asterisks indicate significant differences (**, $P<0.01$) versus the results for control cells. (D) Schematic of the concentration of viral particles from HCV-infected cells using ultracentrifugation. (E) BE-KO1 cells expressing the WT or deletion mutants of ApoE were infected with HCVcc at an MOI of 1. Culture supernatants harvested at 72 h post-infection were concentrated by ultracentrifugation at 32,000 rpm for 2 h at 4°C, and subjected to immunoblotting.
doi:10.1371/journal.ppat.1004534.g008

and ApoH antibodies were purchased from Cell Signaling, ALerCHEK Inc., Abnova, NOVUS Biologicals, and Santa Cruz Biotechnology, respectively. Rat anti-ApoA2 and Sheep anti-ApoC2 antibodies were purchased from R&D systems. Rabbit anti-NS5A antibody was prepared as described previously [54]. Alexa Fluor (AF) 488-conjugated anti-rabbit or mouse IgG antibodies, and AF594-conjugated anti-mouse IgG2a antibodies were purchased from Life Technologies.

Gene silencing

A small interfering RNA (siRNA) pool targeting various apolipoproteins (siGENOME SMARTpool) and control nontar-

geting siRNA were purchased from Dharmacon, and transfected into cells using Lipofectamine RNAi MAX (Life Technologies) according to the manufacturer's protocol. A human shRNA library was purchased from Takara Bio Inc.

Preparation of viruses

Upon transfection of pHH-JFH1-E2p7NS2mt or *in vitro* transcribed TH/JFH1, J6/JFH1 and S310/JFH1 RNA into Huh7.5.1 cells, HCV in the supernatant was collected after serial passages, and infectious titers were determined by a focus-forming assay and expressed in focus-forming units (FFU) [22,23,54]. To compare the localization of core protein, J6/JFH1 was used in Fig. 6E. Pseudoparticles expressing HCV envelope glycoprotein were generated in 293T cells as previously reported [5], and infectivity was assessed by luciferase expression using the Bright-Glo Luciferase assay system (Promega) and expressed in relative light units (RLU).

Lipofection and lentiviral gene transduction

The lentiviral vectors and ViraPower Lentiviral Packaging Mix (Life Technologies) were co-transfected into 293T cells by Trans IT LT-1 (Mirus), and the supernatants were recovered at 48 h post-transfection. The lentivirus titer was determined by the Lenti-XTM qRT-PCR Titration Kit (Clontech), and the expression levels and AcGFP were determined at 48 h post-inoculation.

Immunoblotting

Cells lysed on ice in lysis buffer (20 mM Tris-HCl [pH 7.4], 135 mM NaCl, 1% Triton-X 100, 10% glycerol) supplemented with a protease inhibitor mix (Nacalai Tesque) were boiled in loading buffer and subjected to 5–20% gradient SDS-PAGE. The proteins were transferred to polyvinylidene difluoride membranes (Millipore) and reacted with the appropriate antibodies. The immune complexes were visualized with SuperSignal West Femto Substrate (Pierce) and detected by the LAS-3000 image analyzer system (Fujifilm).

Generation of gene-knockout Huh7 cell lines

Custom ZFN plasmids were designed to bind and cleave the ApoB, ApoE and MTTP genes and were obtained from Sigma Aldrich. Huh7 cells were transfected with *in vitro* transcribed ZFNs mRNA or pX330-MTTP by Lipofectamine 2000 (Life Technologies), and single cell clones were established by the single cell isolation technique. To screen for gene-knockout Huh7 cell clones, mutations in target loci were determined by using a Surveyor assay as previously described [56]. Frameshift of the genes and deficiencies of protein expression were confirmed by direct sequencing and immunoblotting analysis, respectively.

Enzyme-linked immunosorbent assay (ELISA)

Protein concentrations of ApoB or ApoE in the culture supernatants were determined by using ELISA immunoassay kits (Alercheck Inc.) according to the manufacturer's protocol.

Quantitative RT-PCR

Total RNA was extracted from cells by using an RNeasy minikit (Qiagen) and the first-strand cDNA synthesis and qRT-PCR were performed with TaqMan EZ RT-PCR core reagents and a ViiA7 system (Life Technologies), respectively, according to the manufacturer's protocol. The primers for TaqMan PCR targeted to the noncoding region of HCV RNA were synthesized as previously reported [54]. Taqman Gene expression assays were used as the primers and probes targeting to apolipoproteins (Life Technologies). Fluorescent signals were analyzed with the ViiA7 system.

Immunofluorescence assay

Cells cultured on glass slides were fixed with 4% paraformaldehyde (PFA) in phosphate buffered saline (PBS) at room temperature for 30 min, permeabilized for 20 min at room temperature with PBS containing 0.2% Triton after being washed three times with PBS, and blocked with PBS containing 2% FCS for 1 h at room temperature. The cells were incubated with PBS containing the appropriate primary antibodies at room temperature for 1 h, washed three times with PBS, and incubated with PBS containing AF488- or AF594-conjugated secondary antibodies at room temperature for 1 h. For lipid-droplet staining, cells incubated in medium containing 20 μg/ml BODIPY for 20 min at 37°C were washed with pre-warmed fresh medium and incubated for 20 min at 37°C. Cell nuclei were stained with DAPI. Cells were observed with a FluoView FV1000 laser scanning confocal microscope (Olympus).

In vitro transcription, RNA transfection, and colony formation

The plasmid pSGR-JFH1 was linearized with XbaI, and treated with mung bean exonuclease. The linearized DNA was transcribed *in vitro* by using the MEGAscript T7 kit (Life Technologies) according to the manufacturer's protocol. The *in vitro* transcribed RNA (10 μg) was electroporated into Huh7 cells at 10^7 cells/0.4 ml under conditions of 190 V and 975 μF using a Gene Pulser (Bio-Rad) and plated on DMEM containing 10% FCS. The medium was replaced with fresh DMEM containing 10% FCS and 1 mg/ml G418 at 24 h post-transfection. The remaining colonies were cloned by using a cloning ring (Asahi Glass) or fixed with 4% PFA and stained with crystal violet at 4 weeks post-electroporation.

Intracellular infectivity

Intracellular viral titers were determined according to a method previously reported [10]. Briefly, cells were extensively washed with PBS, scraped, and centrifuged for 5 min at 1000× *g*. Cell pellets were resuspended in 500 μl of DMEM containing 10% FCS and subjected to three cycles of freezing and thawing using liquid nitrogen and a thermo block set to 37°C. Cell lysates were centrifuged at 10,000× *g* for 10 min at 4°C to remove cell debris. Cell-associated infectivity was determined by a focus-forming assay.

Electron microscopy and correlative FM-EM analysis

Correlative fluorescence microscopy-electron microscopy (FM-EM) allows individual cells to be examined both in an overview with fluorescence microscopy and in a detailed subcellular-structure view with electron microscopy. Cells infected with HCVcc were examined by the correlative FM-EM method as described previously [57].

Buoyant density fractionation

Culture supernatants of cells infected with HCVcc were concentrated 50 times by using Spin-X UF concentrators (Corning), and the intracellular proteins collected after freeze-and-thaw were applied to the top of a linear gradient formed from 10–40% OptiPrep (Axis-Shield) in PBS and spun at 32,000 rpm for 16 h at 4°C by using an SW41 Ti rotor (Beckman Coulter). Aliquots of 10 consecutive fractions were collected, and the infectious titer and density were determined.

Proteinase K digestion protection assay

The proteinase K digestion protection assay was performed as described previously [37]. Briefly, cells were extensively washed with PBS, scraped, and centrifuged for 5 min at 1000× *g*. The cell pellets were resuspended in 500 μl of PBS and subjected to three cycles of freezing and thawing using liquid nitrogen and a thermo block set to 37°C. The cell lysates were centrifuged at 10,000× *g* for 10 min at 4°C to remove cell debris. The cell lysates were then incubated with 50 μg/ml proteinase K (Life Technologies) in the presence or absence of 5% Triton-X for 1 h on ice, and the digestion was terminated by addition of PMSF (Wako Chemical Industries).

Statistics

The data for statistical analyses are the average of three independent experiments. Results were expressed as the means ± standard deviation. The significance of differences in the means was determined by Student's *t*-test.

Supporting Information

Figure S1 Establishment of ApoB- or ApoE-knockout Huh7 cell lines. Target sequences of ZFNs to ApoB (A) and ApoE (B) are indicated by red characters inside a red box at the top of the panel. Gene knockout by the sequence modification in the 2 alleles of the ApoB (A) or ApoE (B) gene in knockout cell lines (B-KO1 and B-KO2, or E-KO1 and E-KO2) is shown. Deletion and insertion of the sequences are indicated by dotted lines and blue characters in brackets, respectively. Absence of the expressions of ApoB (C) and ApoE (D) in the knockout cell lines was confirmed by immunoblotting using anti-ApoB and -ApoE antibodies. Expression of ApoB (E) and ApoE (F) in the culture supernatants of 293T, Huh7 and the knockout cell lines was determined by ELISA.
(TIF)

Figure S2 Both ApoB and ApoE are involved in the formation of infectious HCV particles. (A) HCVpp were inoculated into Huh7, B-KO1, B-KO2, E-KO1 and E-KO2 cells, and luciferase activities were determined at 48 h post-infection. (B) A subgenomic HCV RNA replicon of the JFH1 strain was electroporated into Huh7, B-KO1 and E-KO1 cells, and colonies were stained with crystal violet at 31 days post-electroporation after selection with 400 μg/ml of G418. HCVcc were inoculated into Huh7, B-KO1, B-KO2, E-KO1 and E-KO2 cells at an MOI of 1 and intracellular HCV RNA at 12, 24, 36 and 60 h post-infection (C), and infectious titers in the culture supernatants at 72 h post-infection (D) were determined by qRT-PCR and focus-forming assay, respectively. (E) Exogenous expression of ApoE in E-KO1 and E-KO2 cells by lentiviral vector was determined by immunoblotting analysis (upper), and infectious titers in the culture supernatants of cells infected with HCVcc at an MOI of 1 were determined at 72 h post-infection by focus-forming assay (lower).
(TIF)

Figure S3 Establishment of ApoB and ApoE double-knockout (BE-KO) Huh7 cell lines. Gene knockout by the ZFN in the 2 alleles of the ApoB and ApoE genes in the double-knockout cell lines, BE-KO1 (A) and BE-KO2 (B), is shown. Deletion and insertion of the sequences are indicated by dotted lines and blue characters in brackets, respectively. (C) The absence of the expressions of ApoB and ApoE in BE-KO1 and BE-KO2 was confirmed by immunoblotting using anti-ApoB and -ApoE antibodies. Expression of ApoB (D) and ApoE (E) in the culture supernatants of 293T, Huh7, BE-KO1 and BE-KO2 cells was determined by ELISA.
(TIF)

Figure S4 Establishment of MTTP-knockout (M-KO) and ApoE and MTTP double-knockout (EM-KO) Huh7 cell lines. (A) Gene knockout by the ZFN in the 2 alleles of the MTTP gene in the knockout cell lines, M-KO1 and M-KO2, is shown. (B) Expression of MTTP in Huh7, M-KO1 and M-KO2 cells was determined by immunoblotting. Expression of ApoB (C) and ApoE (D) in the culture supernatants of Huh7, M-KO1, M-KO2 and 293T cells was determined by ELISA. (E) Gene knockout in the 2 alleles of the MTTP genes by the CRISPR/Cas9 system and in one allele of the ApoE gene by the ZFN in the double-knockout cell lines, EM-KO1 and EM-KO2, is shown. (F) Expression of MTTP in Huh7, EM-KO1 and EM-KO2 cells was determined by immunoblotting. Expression of ApoB (G) and ApoE (H) in the culture supernatants of Huh7, EM-KO1, EM-KO2 and 293T cells was determined by ELISA. (I) Expression of ApoB mRNA in Huh7, M-KO1, M-KO2, EM-KO1, EM-KO2 and 293T cells was determined by qRT-PCR.
(TIF)

Figure S5 Gene silencing of apolipoproteins. BE-KO1 cells infected with HCVcc at an MOI of 1 at 6 h post-transfection with siRNAs targeting ApoA1, ApoA2, ApoC1, ApoC2, ApoC3 and ApoH, and the expression levels of these apolipoproteins were determined by q-RT PCR using specific primers and probes.
(TIF)

Figure S6 ApoD, ApoL1, and ApoO do not participate in the formation of infectious HCV particles. Exogenous expression of ApoD, ApoE, ApoL1 and ApoO in BE-KO1 cells by lentiviral vector was determined by immunoblotting analysis (upper), and infectious titers in the culture supernatants of cells infected with HCVcc at an MOI of 1 were determined at 72 h post-infection by focus-forming assay (lower).
(TIF)

Figure S7 BE-KO1 cells permit propagation of JEV and DENV. Huh7, BE-KO1 and ApoE-restored (ApoE-res) cells were infected with JEV and DENV at an MOI of 0.1, and infectious titers in the culture supernatants were determined by focus-forming assay at 48 h post-infection.
(TIF)

Figure S8 Localization of core, NS5A proteins and ER in BE-KO Huh7 cells. BE-KO1 cells infected with HCVcc at an MOI of 1 were subjected to immunofluorescence analyses by using antibodies against core, NS5A and Calnexin.
(TIF)

Acknowledgments

We thank M. Tomiyama for her secretarial work and M. Ishibashi and Y. Sugiyama for their technical assistance. We also thank M. Hijikata, T. Wakita, R. Bartenschlager, F. Chisari, and M. Whitt for providing experimental materials.

Author Contributions

Conceived and designed the experiments: TF SN MY IS TW KK YM. Performed the experiments: TF MW CO MS SY TM. Analyzed the data: TF MW SN TO DO YM. Contributed reagents/materials/analysis tools: KK YM. Wrote the paper: TF SN DO YM.

References

1. Maasoumy B, Wedemeyer H (2012) Natural history of acute and chronic hepatitis C. Best. Pract. Res. Clin. 26: 410–412.
2. Jacobson IM, McHutchison JG, Dusheiko G, Di Bisceglie AM, Reddy KR, et al. (2011) Telaprevir for previously untreated chronic hepatitis C virus infection. N. Engl. J. Med. 364: 2405–2416.
3. Sulkowski MS, Gardiner DF, Rodriguez-Torres M, Reddy KR, Hassanein T, et al. (2014) Daclatasvir plus Sofosbuvir for previously treated or untreated chronic HCV infection. N. Engl. J. Med. 370: 211–221.
4. Janssen HL, Reesink HW, Lawitz EJ, Zeuzem S, Rodriguez-Torres M, et al. (2013) Treatment of HCV infection by targeting microRNA. N. Engl. J. Med. 368: 1685–1694.
5. Bartosch B, Dubuisson J, Cosset F (2003) Infectious hepatitis C virus pseudo-particles containing functional E1–E2 envelope protein complexes. J. Exp. Med. 197: 633–642.
6. Lohmann V, Korner F, Koch JO, Herian U, Theilmann L, et al. (1999) Replication of subgenomic hepatitis C virus RNAs in a hepatoma cell line. Science. 285: 110–113.
7. Wakita T, Pietschmann T, Kato T, Date T, Miyamoto M, et al. (2005) Production of infectious hepatitis C virus in tissue culture from a cloned viral genome. Nat. Med. 11: 791–796.
8. Lindenbach BD, Evans MJ, Syder AJ, Wolk B, Tellinghuisen TL, et al. (2005) Complete replication of hepatitis C virus in cell culture. Science. 309: 623–626.
9. Jirasko V, Montserret R, Lee JY, Gouttenoire J, Moradpour D, et al. (2010) Structural and functional studies of nonstructural protein 2 of the hepatitis C virus reveal its key role as organizer of virion assembly. PLoS Pathog. 6: e1001233.
10. Gastaminza P, Cheng G, Wieland S, Zhong J, Liao W, et al. (2008) Cellular determinants of hepatitis C virus assembly, maturation, degradation, and secretion. J. Virol. 82: 2120–2129.
11. Jiang J, Luo G (2009) Apolipoprotein E but not B is required for the formation of infectious hepatitis C virus particles. J. Virol. 83: 12680–12691.
12. Andre P, Komurian-Pradel F, Deforges S, Perret M, Berland L, et al. (2002) Characterization of Low- and Very-Low-Density hepatitis C virus RNA-containing particles. J. Virol. 76: 6919–6928.
13. Saito H, Lund-Katz S, Phillips MC. (2004) Contribution of domain structure and lipid interaction to the functionality of exchangeable human apolipoproteins. Prog. Lipid Res. 43: 350–380.
14. Narayanaswami V, Kiss RS, Weers PM. (2010) The helix bundle: A reversible lipid binding motif. Comp. Biochem. Physiol. A Mol. Integr. Physiol. 155: 123–133.
15. Mancone C, Steindler C, Santangelo L, Simonte G, Vlassi C, et al. (2011) Hepatitis C virus production requires apolipoprotein A-1 and affects its association with nascent low-density lipoproteins. Gut. 60: 378–386.
16. Da Costa D, Turek M, Felmlee DJ, Girardi E, Pfeffer S, et al. (2012) Reconstitution of the entire hepatitis C virus life cycle in nonhepatic cells. J. Virol. 86: 11919–11925.
17. Porteus MH, Carroll D (2005) Gene targeting using zinc finger nucleases. Nat. Biotechnol. 23: 967–973.
18. Zhang F, Cong L, Lodato S, Kosuri S, Church GM, et al. (2011) Efficient construction of sequence-specific TAL effectors for modulating mammalian transcription. Nat. Biotechnol. 29: 149–153.
19. Mali P, Yang L, Esvelt KM, Aach J, Guell M, et al. (2013) RNA-guided human genome engineering via Cas9. Science. 339: 823–826.
20. Kupershmidt I, Su QJ, Grewal A, Sundaresh S, Halperin I, et al. (2010) Ontology-based meta-analysis of global collections of high-throughput public data. PLoS One. 5: e13066.
21. Hussain MM, Shi J, Dreizen P (2003) Microsomal triglyceride transfer protein and its role in apoB-lipoprotein assembly. J. Lipid Res. 44: 22–32.
22. Takebe Y, Saucedo CJ, Lund G, Uenishi R, Hase S, et al. (2013) Antiviral lectins from Red and Blue-Green Algae show potent *in vitro* and *in vivo* activity against hepatitis C virus. PLoS One. 8: e64449.
23. Kim S, Date T, Yokokawa H, Kono T, Aizaki H, et al. (2014) Development of hepatitis C virus genotype 3a cell culture system. Hepatology. doi: 10.1002/hep.27197.
24. Miyanari Y, Atsuzawa K, Usuda N, Watashi K, Hishiki T, et al. (2007) The lipid droplet is an important organelle for hepatitis C virus production. Nat. Cell Biol. 9: 961–969.
25. Boson B, Granio O, Bartenschlager R, Cosset F (2011) A concerted action of hepatitis C virus p7 and nonstructural protein 2 regulates core localization at the endoplasmic reticulum and virus assembly. PLoS Pathog. 7: e1002144.
26. Gentzsch J, Brohm C, Steinmann E, Friesland M, Menzel N, et al. (2013) Hepatitis C virus p7 is critical for capsid assembly and envelopment. PLoS Pathog. 9: e1003355.
27. Shavinskaya A, Boulant S, Penin F, McLauchlan J, Bartenschlager R. (2007) The lipid droplet binding domain of hepatitis C virus core protein is a major determinant for efficient virus assembly. J. Biol. Chem. 282: 37158–37169.
28. Ai L, Lee Y, Chen SS (2009) Characterization of hepatitis C virus core protein multimerization and membrane envelopment: revelation of a cascade of core-membrane interactions. J. Virol. 83: 9923–9939.
29. Mei X, Atkinson D (2011) Crystal structure of C-terminal truncated apolipoprotein A-1 reveals the assembly of high density lipoprotein (HDL) by dimerization. J. Biol. Chem. 286: 38570–38582.
30. Rozek A, Sparrow JT, Weisgraber KH, Cushley JR (1999) Conformation of human apolipoprotein C-1 in a lipid-mimetic environment determined by CD and NMR spectrometry. Biochemistry. 38: 14475–14484.
31. Eichinger A, Nasreen A, Jin H (2007) Structural insight into the dual ligand specificity and mode of high density lipoprotein association of apolipoprotein D. J. Biol. Chem. 282: 31068–31075.
32. Chen J, Li Q, Wang J (2011) Topology of human apolipoprotein E3 uniquely regulates its diverse biological functions. Proc. Natl. Acad. Sci. U. S. A. 108: 14813–14818.
33. Schwarzenbacher R, Zeth K, Diederichs K, Gries A, Kostner GM, et al. (1999) Crystal structure of human β2-glycoprotein 1: implication for phospholipid binding and the antiphospholipid syndrome. EMBO J. 18: 6228–6239.
34. Sevvana M, Kassler K, Ahnstrom J, Weiler S, Dahlback B, et al. (2010) Mouse ApoM displays an unprecedented seven-stranded lipocalin fold: folding decoy or alternative native fold? J. Mol. Biol. 404: 363–371.
35. Nielsen SU, Bassendine MF, Burt AD, Martin C, Pumeechockchai W, et al. (2006) Association between hepatitis C virus and very-low-density lipoprotein (VLDL)/LDL analyzed in iodixanol density gradients. J. Virol. 80: 2418–2428.
36. Jammart B, Michelet M, Pecheur E, Parent R, Bartosch B, et al. (2013) Very-low-density lipoprotein (VLDL)-prpducing and hepatitis C virus-replicating HepG2 cells secrete no more lipoviroparticles than VLDL-deficient Huh7.5 cells. J. Virol. 87: 1405–1412.
37. Hueging K, Doepke M, Vieyres G, Bankwitz D, Frentzen A, et al. (2014) Apolipoprotein E codetermines tissue tropism of hepatitis C virus and is crucial for viral cell-to-cell transmission by contributing to a postenvelopment step of assembly. J. Virol. 88: 1433–1466.
38. Coller KE, Heaton NS, Berger KL, Cooper JD, Saunders JL, et al. (2012) Molecular determinants and dynamics of hepatitis C virus secretion. PLoS Pathog. 8: e1002466.
39. Catanese TM, Uryu K, Kopp M, Edwards TJ, Andrus L, et al. (2013) Ultrastructural analysis of hepatitis C virus particles. Proc. Natl. Acad. Sci. U. S. A. 110: 9505–9510.
40. Cheng G, Montero A, Gastaminza P, Whitten-Bauer C, Wieland SF, et al. (2008) A virocidal amphipathic α-helical peptide that inhibits hepatitis C virus infection *in vitro*. Proc. Natl. Acad. Sci. U. S. A. 105: 3088–3093.
41. Scarselli E, Ansuini H, Cerino R, Roccasecca RM, Acali S, et al. (2002) The human scavenger receptor class B type 1 is a novel candidate receptor for the hepatitis C virus. EMBO J. 21: 5017–5025.
42. Molina S, Castet V, Fournier-Wirth C, Pichard-Garcia L, Avner R, et al. (2007) The low-density lipoprotein receptor plays a role in the infection of primary human hepatocytes by hepatitis C virus. J. Hepatol. 46: 411–419.
43. Owen DM, Huang H, Ye J, Gale MJ (2009) Apolipoprotein E on hepatitis C virion facilitates infection through interaction with low-density lipoprotein receptor. Virology. 394: 99–108.
44. Prentoe J, Serre SB, Ramirez S, Nicosia A, Gottwein JM, et al. (2014) Hypervariable region 1 deletion and required adaptive envelope mutations confer decreased dependency on scavenger receptor class B type 1 and low density lipoprotein receptor for hepatitis C virus. J. Virol. 88: 1725–1739.
45. Meunier J, Russell RS, Engle RE, Faulk KN, Purcell RH, et al. (2008) Apolipoprotein C1 association with hepatitis C virus. J. Virol. 82: 9647–9656.
46. Dreux M, Boson B, Ricard-Blum S, Molle J, Lavillette D et al. (2007) The exchangeable apolipoprotein ApoC-1 promotes membrane fusion of hepatitis C virus. J. Biol. Chem. 282: 32357–32369.
47. Fukuhara T, Matsuura Y (2013) Role of miR-122 and lipid metabolism in HCV infection. J. Gastroenterol. 48: 169–176.
48. Ploss A, Evans MJ, Gaysinskaya VA, Panis M, You H, et al. (2009) Human occludin is a hepatitis C virus entry factor required for infection of mouse cells. Nature. 457: 882–886.
49. Mercer DF, Schiller DE, Elliott JF, Douglas DN, Hao C, et al. (2001) Hepatitis C virus replication in mice with chimeric human livers. Nat. Med. 7: 927–933.
50. Dorner M, Horwitz JA, Donovan BM, Labitt RN, Budell BC, et al. (2013) Completion of the entire hepatitis C virus life cycle in genetically humanized mice. Nature. 501: 237–241.
51. Wang H, Yang H, Shivalila CS, Dawlaty MM, Cheng AW, et al. (2013) One-step generation of mice carrying mutations in multiple genes by CRISPR/Cas-mediated genome engineering. Cell. 153: 910–918.
52. Cho SW, Kim S, Kim JM, Kim J (2013) Targeted genome engineering in human cells with the Cas9 RNA-guided endonuclease. Nat. Biotechnol. 31: 230–232.
53. Shalem O, Sanjana NE, Hartenian E, Shi X, Scott DA, et al. (2014) Genome-scale CRISPR-Cas9 knockout screening in human cells. Science. 343: 84–87.
54. Fukuhara T, Kambara H, Shiokawa M, Ono C, Katoh H, et al. (2012) Expression of microRNA miR-122 facilitates an efficient replication in nonhepatic cells upon infection with hepatitis C virus. J. Virol. 86: 7918–7933.
55. Russell RS, Meunier JC, Takikawa S, Faulk K, Engle RE, et al. Advantages of a single-cycle production assay to study cell culture-adaptive mutations of hepatitis C virus. Proc. Natl. Acad. Sci. U. S. A. 105: 4370–4375 (2008).
56. Guschin YD, Waite AJ, Katibah GE, Miller JC, Holmes MC, et al. (2010) A rapid and general assay for monitoring endogenous gene modification. Methods Mol. Biol. 649: 247–256 (2010).
57. Rieder CL, Bowser SS (1985). Correlative immunofluorescence and electron microscopy on the same section of epon-embedded material. J. Histochem. Cytochem. 33: 165–171.

JVI
Journals.ASM.org

Novel Permissive Cell Lines for Complete Propagation of Hepatitis C Virus

Mai Shiokawa,[a] Takasuke Fukuhara,[a] Chikako Ono,[a] Satomi Yamamoto,[a] Toru Okamoto,[a] Noriyuki Watanabe,[b] Takaji Wakita,[b] Yoshiharu Matsuura[a]

Department of Molecular Virology, Research Institute for Microbial Diseases, Osaka University, Osaka, Japan[a]; Department of Virology II, National Institute of Infectious Diseases, Tokyo, Japan[b]

ABSTRACT

Hepatitis C virus (HCV) is a major etiologic agent of chronic liver diseases. Although the HCV life cycle has been clarified by studying laboratory strains of HCV derived from the genotype 2a JFH-1 strain (cell culture-adapted HCV [HCVcc]), the mechanisms of particle formation have not been elucidated. Recently, we showed that exogenous expression of a liver-specific microRNA, miR-122, in nonhepatic cell lines facilitates efficient replication but not particle production of HCVcc, suggesting that liver-specific host factors are required for infectious particle formation. In this study, we screened human cancer cell lines for expression of the liver-specific α-fetoprotein by using a cDNA array database and identified liver-derived JHH-4 cells and stomach-derived FU97 cells, which express liver-specific host factors comparable to Huh7 cells. These cell lines permit not only replication of HCV RNA but also particle formation upon infection with HCVcc, suggesting that hepatic differentiation participates in the expression of liver-specific host factors required for HCV propagation. HCV inhibitors targeting host and viral factors exhibited different antiviral efficacies between Huh7 and FU97 cells. Furthermore, FU97 cells exhibited higher susceptibility for propagation of HCVcc derived from the JFH-2 strain than Huh7 cells. These results suggest that hepatic differentiation participates in the expression of liver-specific host factors required for complete propagation of HCV.

IMPORTANCE

Previous studies have shown that liver-specific host factors are required for efficient replication of HCV RNA and formation of infectious particles. In this study, we screened human cancer cell lines for expression of the liver-specific α-fetoprotein by using a cDNA array database and identified novel permissive cell lines for complete propagation of HCVcc without any artificial manipulation. In particular, gastric cancer-derived FU97 cells exhibited a much higher susceptibility to HCVcc/JFH-2 infection than observed in Huh7 cells, suggesting that FU97 cells would be useful for further investigation of the HCV life cycle, as well as the development of therapeutic agents for chronic hepatitis C.

More than 170 million individuals worldwide are infected with hepatitis C virus (HCV), and the cirrhosis and hepatocellular carcinoma induced by HCV infection are life-threatening diseases (1). Current standard therapy combining pegylated-interferon (peg-IFN) and ribavirin (RBV) has achieved a sustained virological response (SVR) in 50% of individuals infected with HCV genotype 1 (2). Recently, directly acting antiviral (DAA) agents have been applied in a clinical setting (3). An SVR rate of over 80% has been realized by combination therapy with peg-IFN, RBV, and NS3/4A inhibitors in genotype 1 patients (4, 5). In addition, several DAAs, including inhibitors for NS3/4A protease, NS5A, and NS5B polymerase, are currently in clinical trials. Several reports have shown that *in vitro* replication of HCV RNA is significantly inhibited by treatment with daclatasvir (NS5A inhibitor) and asunaprevir (NS3 protease inhibitor), and these two DAAs are also effective for patients infected with genotype 1 HCV who showed no response to previous therapy with peg–IFN-α and RBV (6–8). On the other hand, it has been shown that drug-resistant breakthrough viruses emerge during treatment with DAAs (9–12). Therefore, identification of host factors crucial for the propagation of HCV is an important task for the development of novel therapeutics for chronic hepatitis C with a low frequency of emergence of drug-resistant viruses.

The establishment of an *in vivo* infection model has been hampered by the narrow host range and tissue tropism of HCV. Although chimpanzees are the only experimental animals susceptible to HCV infection, it is difficult to use a chimpanzee model of experimental infection due to ethical concerns (13, 14). In addition, *in vitro* infection models have also been restricted to the combination of cell culture-adapted clones based on the genotype 2a JFH-1 strain (HCVcc) and human hepatoma cell lines, including Huh7 (15). Recently, several reports have shown that the exogenous expression of microRNA-122 (miR-122) facilitates the efficient propagation of HCVcc in HepG2 and Hep3B cells, which are nonpermissive for propagation of HCVcc (16, 17). Furthermore, we reported that nonhepatic cell lines, including Hec1B cells derived from uterine endometrial adenocarcinoma, also permit replication of HCV RNA by exogenous expression of miR-122 (18). These reports indicate that miR-122 is one of the most important determinants for liver tropism of HCV infection. Interestingly, formation of infectious particles was not observed in

Received 26 December 2013 Accepted 25 February 2014
Published ahead of print 5 March 2014
Editor: T. S. Dermody
Address correspondence to Yoshiharu Matsuura, matsuura@biken.osaka-u.ac.jp.
Copyright © 2014, American Society for Microbiology. All Rights Reserved.
doi:10.1128/JVI.03839-13

Downloaded from http://jvi.asm.org/ on February 12, 2015 by OSAKA UNIV BIKEN MI

spite of efficient replication of HCV RNA in nonhepatic cells, suggesting that liver-specific factors other than miR-122 are involved in HCV assembly. Previous reports suggested that very-low-density lipoprotein (VLDL)-associated proteins, including apolipoprotein B (ApoB), apolipoprotein E (ApoE), and microsomal triglyceride transfer protein (MTTP), play important roles in infectious particle production of HCV (19–23). In addition, Miyanari et al. indicated that lipid droplets (LDs) are crucial organelles for HCV particle assembly (24). These reports suggest that liver-specific lipid metabolism and liver-specific host factors closely participate in assembly of HCV.

Cancer cells are classified into well-differentiated and intermediately and poorly differentiated stages, and these stages have been shown to be strongly related to cancer behaviors, with an immature tumor generally being more aggressive than its more differentiated counterpart. Thus, it is believed that well-differentiated cancer cells maintain the tissue-specific cellular functions and exhibit morphology similar to that of normal cells (25). Permissive cell lines for HCV propagation, including Huh7, HepG2, and Hep3B cells, are derived from well-differentiated hepatocellular carcinoma (HCC) (26, 27). In addition, recent reports indicated that hepatocyte-like cells derived from induced pluripotent stem cells (iPS cells/iPSCs) express high levels of miR-122 and VLDL-associated proteins and support propagation of HCVcc (28–30). These results suggest that the hepatic differentiation required for hepatic functions is involved in HCV propagation.

In this study, we identified novel cell lines supporting complete propagation of HCVcc by screening cancer cell lines expressing α-fetoprotein (AFP), which is highly expressed in well-differentiated hepatocellular carcinoma and evaluated in most cancer cell lines (31). These cells exhibit high levels of expression of liver-specific host factors and permit complete propagation of HCVcc without any exogenous expression of liver-specific factors, including receptor molecules, miR-122, and apolipoproteins. Our current study suggests that hepatic differentiation participates in the expression of liver-specific host factors required for complete propagation of HCV.

MATERIALS AND METHODS

NextBio Body Atlas. The NextBio Body Atlas application allows the aggregated analysis of gene expression across various normal tissues, normal cell types, and cancer cell lines. It enables us to investigate the expression of individual genes as well as gene sets. Samples for Body Atlas data are obtained from publicly available studies that are internally curated, annotated, and processed (32). Body Atlas measurements are generated from all available RNA expression studies that used Affymetrix U133 Plus or U133A Genechip arrays for human studies. The results for 128 human tissue samples from 1,067 arrays, those for 157 human cell types from 1,474 arrays, and those for 359 human cancer cell lines from 376 arrays are incorporated. In this study, we screened cell lines expressing a high level of AFP. The details of the analysis protocol developed by NextBio were described previously (32). The raw data used in this application are derived from the GSK Cancer Cell Line data deposited at the National Cancer Institute website (https://array.nci.nih.gov/caarray/project/woost-00041).

Plasmids. The cDNA clones of pri-miR-122 and *Aequorea coerulescens* green fluorescent protein (AcGFP) were inserted between the XhoI and XbaI sites of lentiviral vector pCSII-EF-RfA, which was provided by M. Hijikata, and the resulting plasmids were designated pCSII-EF-miR-122 and pCSII-EF-AcGFP, respectively. Plasmids pHH-JFH1-E2p7NS2mt, encoding a cDNA of a full-length RNA of the JFH-1 strain, and pJFH2/AS/mtT4, encoding a cDNA of a full-length RNA of the JFH-2 strain, were described previously (33, 34). pSGR-Con1, which encodes a subgenomic replicon (SGR) of the Con1 strain, was provided by R. Bartenschlager. pIFN-β-Luc and pISRE-Luc carrying a firefly luciferase (Luc) gene under the control of the IFN-β- and IFN-sensitive response element (ISRE) promoters, respectively, were provided by S. Akira. The internal control plasmid encoding a *Renilla* luciferase (pRL-SV40) was purchased from Promega (Madison, WI). The plasmids used in this study were confirmed by sequencing with an ABI Prism 3130 genetic analyzer (Applied Biosystems, Tokyo, Japan).

Cell lines. All cell lines were cultured at 37°C under the conditions of a humidified atmosphere and 5% CO_2. Human hepatocellular carcinoma-derived Huh7, Hep3B, HepG2, and JHH-4 (JCRB0435) cells, embryonic kidney-derived 293T cells, gastric cancer-derived FU97 (JCRB1074) cells, and ovarian adenocarcinoma-derived OV-90 cells were maintained in Dulbecco's modified Eagle's medium (DMEM; Sigma-Aldrich, St. Louis, MO) supplemented with 100 U/ml penicillin, 100 μg/ml streptomycin, and 10% fetal calf serum (FCS). JHH-4 and FU97 cells were obtained from the Japanese Collection of Research Bioresources (JCRB) Cell Bank. OV-90 cells were obtained from the American Type Culture Collection (ATCC). 293T-CLDN cells stably expressing claudin-1 (CLDN1) were established by the introduction of expression plasmid pCAG-pm3 encoding CLDN1 under the control of the CAG promoter. The Huh7-derived cell line Huh7.5.1 was provided by F. Chisari. Huh7 and FU97 cells harboring the SGR of the Con1 strain (Con1-SGR) were prepared as described previously (35) and maintained in DMEM containing 1 mg/ml and 400 μg/ml of G418 (Nacalai Tesque, Kyoto, Japan), respectively.

Preparation of viruses. HCVs derived from the genotype 2a JFH-1 strain (HCVcc) were prepared after serial passages of the culture supernatants of Huh7.5.1 cells transfected with pHH-JFH1-E2p7NS2mt into Huh7.5.1 cells (33). HCVs derived from the genotype 2a JFH-2 strain (HCVcc/JFH-2) were prepared by several passages of the culture supernatants of Huh7.5.1 cells electroporated with JFH-2 RNA transcribed *in vitro*. Infectious titers were determined by a focus-forming assay and expressed as focus-forming units (FFU) (15). The vesicular stomatitis virus (VSV) variant NCP12.1 derived from the Indiana strain was provided by M. Whitt. Pseudotype VSVs bearing HCV E1 and E2 glycoproteins (HCVpv), were prepared as described previously (36), and infectivity was assessed by a luciferase assay system (Promega) according to a protocol provided by the manufacturer and expressed in relative light units (RLU).

Antibodies and drugs. Mouse monoclonal antibodies to HCV nonstructural protein 5A (NS5A) and β-actin were purchased from Austral Biologicals (San Ramon, CA) and Sigma-Aldrich, respectively. Rabbit anti-HCV core protein was prepared as described previously (37). Mouse anti-E2 polyclonal antibody was also prepared (unpublished data). Anti-human CD81 (hCD81) monoclonal antibody (JS-81) and rabbit anti-scavenger receptor class B type 1 (SR-BI) antibody were purchased from BD Biosciences (Franklin Lakes, NJ) and Novus Biologicals (Littleton, CO), respectively. Rabbit anti-CLDN1 and anti-occludin (OCLN) antibodies, Alexa Fluor 488 (AF488)-conjugated anti-rabbit and -mouse IgG antibodies, and AF594-conjugated anti-rabbit IgG antibodies were purchased from Life Technologies (Carlsbad, CA). Rabbit anti-signal transducer and activators of transcription 2 (STAT2) antibody and anti-calregulin antibody were purchased from Santa Cruz (Santa Cruz, CA). Rabbit anti-IFN regulatory factor 3 (IRF3) antibody was purchased from Abcam (Cambridge, United Kingdom). Phycoerythrin (PE)-conjugated anti-hCD81 and anti-mouse IgG antibodies were purchased from BD Biosciences. Anti-ApoB horseradish peroxidase (HRP)-conjugated antibody was purchased from ALerCHEK (Springvale, ME). The HCV NS3/4A protease inhibitor was purchased from Acme Bioscience (Salt Lake City, UT). Human recombinant alpha IFN (IFN-α) was purchased from PBL Biomedical Laboratories (Piscataway, NJ). BODIPY558/568 lipid probe and 4′, 6-diamidino-2-phenylindole (DAPI) were purchased from Life Technologies and Vector Laboratories, Inc. (Burlingame, CA), respectively. Cyclosporine and CP-346086 were purchased from Sigma-Aldrich. Ribavirin (RBV) was purchased from Tokyo Chemical Industry

Downloaded from http://jvi.asm.org/ on February 12, 2015 by OSAKA UNIV BIKEN MI

(Tokyo, Japan). BMS-790052 and PSI-7977 were purchased from Shanghai Haoyuan Chemexpress (Shanghai, China). BMS-200150 was purchased from ChemStep (Martillac, France). The locked nucleic acid (LNA) targeted to miR-122, miR-122–LNA (5′-CcAttGTcaCaCtCC-3′), and its negative control, control-LNA (Ctrl-LNA) (5′-CcAttCTgaCcCtA C-3′), were purchased from Gene Design (Osaka, Japan); LNAs and DNAs are indicated in capital and lowercase letters, respectively. Sulfur atoms in oligonucleotide phosphorothioates are substituted for nonbridging oxygen atoms. The capital C indicates LNA methylcytosine.

Transfection and lentiviral gene transduction. Cells were transfected with the plasmids by using TransIT LT-1 transfection reagents (Mirus, Madison, WI) according to the manufacturer's protocol. LNAs were introduced into cells by Lipofectamine RNAi MAX (Life Technologies). The lentiviral vectors and ViraPower lentiviral packaging mix (Life Technologies) were cotransfected into 293T cells, and the supernatants were recovered at 48 h posttransfection. The lentivirus titer was determined by a lenti-XTM quantitative reverse transcription-PCR (qRT-PCR) titration kit (Clontech, Mountain View, CA), and the expression levels of miR-122 and AcGFP were determined at 48 h postinoculation.

Quantitative RT-PCR. HCV RNA levels were determined by a method described previously (38). Total RNA was extracted from cells by using an RNeasy minikit (Qiagen, Valencia, CA), and the first-strand cDNA synthesis and qRT-PCR were performed with TaqMan EZ RT-PCR core reagents and a ViiA7 system (Life Technologies), respectively, according to the manufacturer's protocol. The primers for TaqMan PCR targeted to the noncoding region of HCV RNA were synthesized as previously reported (39). To determine the expression of miR-122, total miRNAs were prepared by using an miReasy minikit (Qiagen), and miR-122 was determined by using the fully processed miR-122-specific RT and PCR primers provided in the TaqMan microRNA assays (Life Technologies) according to the manufacturer's protocol. U6 small nuclear RNA was used as an internal control. Fluorescent signals were analyzed with the ViiA7 system.

Immunoblotting. Cells were lysed on ice in lysis buffer (20 mM Tris-HCl [pH 7.4], 135 mM NaCl, 1% Triton X-100, 10% glycerol) supplemented with a protease inhibitor mix (Nacalai Tesque). Culture supernatants of cells incubated for 3 days were used for detection of ApoB. The samples were boiled in loading buffer and subjected to a 5% to 20% gradient SDS-PAGE or 3 to 8% Tris-acetate gel (Thermo Scientific, Waltham, MA). The proteins were transferred to polyvinylidene difluoride membranes (Millipore, Bedford, MA) and reacted with the appropriate antibodies. The immune complexes were visualized with SuperSignal West Femto substrate (Pierce, Rockford, IL) and detected with an LAS-3000 image analyzer system (Fujifilm, Tokyo, Japan).

Immunofluorescence assay. Cells cultured on glass slides were fixed with 4% paraformaldehyde (PFA) in phosphate-buffered saline (PBS) at room temperature for 30 min, permeabilized for 20 min at room temperature with PBS containing 0.2% Triton X-100, washed three times with PBS, and blocked with PBS containing 2% FCS for 1 h at room temperature. Then cells were incubated with PBS containing appropriate primary antibodies at room temperature for 1 h, washed three times with PBS, and incubated with PBS containing AF488- or AF594-conjugated secondary antibodies at room temperature for 45 min. For lipid droplet staining, cells were incubated in medium containing 20 μg/ml BODIPY for 20 min at 37°C, washed with prewarmed fresh medium, and incubated for 20 min at 37°C. The stained cells were covered with Vectashield Mounting Medium containing DAPI (Vector Laboratories Inc., Burlingame, CA) and observed with a FluoView FV1000 laser scanning confocal microscope (Olympus, Tokyo, Japan).

***In vitro* transcription, RNA transfection, and colony formation.** The plasmid pSGR-Con1 was linearized with ScaI and transcribed *in vitro* by using a MEGAscript T7 kit (Life Technologies) according to the manufacturer's protocol. The *in vitro*-transcribed RNA (10 μg) was electroporated into FU97 cells at 10^7 cells/0.4 ml under conditions of 210 V and 960 μF using a Gene Pulser apparatus (Bio-Rad, Hercules, CA) and plated on DMEM containing 10% FCS. The medium of FU97 cells was replaced with fresh DMEM containing 10% FCS and 400 μg/ml G418 at 24 h postelectroporation. The remaining colonies were cloned by using a cloning ring (Asahi Glass, Tokyo, Japan) or fixed with 4% PFA in PBS and stained with crystal violet at 5 weeks postelectroporation.

Flow cytometry. Cultured cells were detached with 0.25% trypsin-EDTA, incubated with PE-conjugated anti-hCD81 antibody or anti-mouse IgG antibody for 1 h at 4°C, washed twice with PBS containing 1% bovine serum albumin (BSA), and analyzed by using a flow cytometry system (FACSCalibur; BD Biosciences).

Gene silencing. A commercially available small interfering RNA (siRNA) pool targeting ApoB and ApoE (siGENOME SMARTpool human ApoB and ApoE) and a control nontargeting siRNA were purchased from Dharmacon (Buckinghamshire, United Kingdom) and transfected into JHH-4 and FU97 cells using Lipofectamine RNAi MAX (Life Technologies) according to the manufacturer's protocol.

Luciferase assay. Cells seeded onto 24-well plates at a concentration of 5×10^4 cells/well were transfected with 250 ng of each of the plasmids, stimulated with the appropriate ligands for 24 h at 24 h posttransfection, and lysed in 100 μl of passive lysis buffer (Promega). Luciferase activity was measured in 20-μl aliquots of the cell lysates using a dual-luciferase reporter assay system (Promega). Firefly luciferase activity was standardized with that of *Renilla* luciferase cotransfected with the internal control plasmid pRL-SV40 and was expressed in RLU.

Neutralization assay. Huh7, JHH-4, and FU97 cells were pretreated with 10 μg/ml of anti-hCD81 (JS-81) monoclonal antibody for 1 h at 37°C and then inoculated with HCVcc (1×10^6 FFU/ml). Anti-E2 monoclonal antibody (10 μg/ml) was incubated with HCVcc (1×10^6 FFU/ml) for 1 h and then inoculated into cells. Intracellular HCV RNA levels at 12, 24, 48, and 72 h postinfection were determined by qRT-PCR.

Buoyant density gradient analysis. Culture supernatants of Huh7.5.1 and FU97 cells infected with HCVcc at 72 h postinfection were passed through 0.45-μm-pore-size filters and concentrated by a Spin-X Concentrator (100,000-molecular-weight cutoff column; Corning, Lowell, MA). One milliliter of concentrated sample was layered onto the top of a linear gradient formed from 10% to 40% of OptiPrep (Axis-Shield PoC, Oslo, Norway) in PBS and spun at 32,000 rpm for 16 h at 4°C by using an SW41-Ti rotor (Beckman Coulter, Fullerton, CA). Each fraction collected from the top was analyzed by qRT-PCR, focus-forming assay, and immunoblotting.

Statistical analysis. The data for statistical analyses are the averages of three independent experiments. Results were expressed as the means ± standard deviations. The significance of differences in the means was determined by Student's *t* test.

RESULTS

JHH-4 and FU97 cells express high levels of the liver-specific host factors required for HCV propagation. AFP is known as a marker for not only well-differentiated HCC (31) but also the early stage of differentiation to hepatocytes in embryonic stem (ES)/iPS cells (29, 40, 41). Generally, well-differentiated cancer cells show better maintenance of their cell-specific functions than poorly differentiated cancer cells. Therefore, we hypothesized that cancer cell lines with high levels of AFP expression retain sufficient hepatic function for HCV propagation. To examine this hypothesis, we first screened cancer cell lines by using the NextBio Body Atlas application and identified the following cell lines that expressed high levels of AFP: Takigawa and FU97 cells derived from gastric cancer, HepG2 and Hep3B cells from hepatocellular carcinoma, Caco-2 cells from colon cancer, and OV-90 cells from ovarian cancer. To evaluate the correlation of AFP expression with the hepatic functions in these cell lines, we examined the expression of liver-specific host factors, including albumin (ALB), ApoB, and ApoE, by using the Web-based NextBio search engine and found

Downloaded from http://jvi.asm.org/ on February 12, 2015 by OSAKA UNIV BIKEN MI

that these cell lines expressed higher levels of the liver-specific genes than the HEK293 cells used as negative controls (Fig. 1A). These results suggested that the expression of AFP was correlated with that of the examined liver-specific host factors in cancer cell lines. Next, to confirm this correlation, the expression levels of ALB, ApoB, ApoE, MTTP, and miR-122 were determined by qPCR in AFP-expressing cell lines, including FU97, OV-90, and HCC-derived Huh7, HepG2, Hep3B, and JHH-4 cells (Fig. 1B). Takigawa cells were difficult to culture, and Caco-2 cells have previously been reported to permit entry and replication of HCV (42, 43); therefore, we excluded these cell lines for further analyses. JHH-4 cells were previously shown to permit a partial propagation of HCV in a three-dimensional cultivation by using a radial-flow bioreactor system upon inoculation with plasma from an HCV carrier (44). In contrast to 293T cells, these AFP-expressing cell lines express high levels of the examined liver-specific host factors, suggesting that these cell lines maintain their hepatic functions. Because previous studies have shown that Huh7, HepG2, and Hep3B cells are susceptible to HCVcc infection, we selected JHH-4, FU97, and OV-90 cells for further investigation as new cell line candidates for HCV propagation. It is well known that hepatocytes and intestinal cells produce ApoB100 and ApoB48, respectively. ApoB100 was detected in the culture supernatants of Huh7, JHH-4, FU97, and OV-90 cells but not in those of 293T cells by immunoblotting (Fig. 1C). These results suggest that FU97 and OV-90 cells are differentiated into hepatocyte-like cells and possess liver-specific functions. The expression of entry receptor molecules for HCV, including hCD81, CLDN1, OCLN, and SR-BI (45–48), in these cell lines was confirmed by immunoblotting and fluorescence-activated cell sorting (FACS) analyses (Fig. 1D and E). To further determine the authenticity of the receptor candidates for HCV entry, HCVpv was inoculated into these cell lines. Although the infectivity of HCVpv to JHH-4 and FU97 cells was comparable to that in Huh7 cells, OV-90 cells did not show any susceptibility to HCVpv infection (Fig. 1F). Cell surface expression of CLDN1 and OCLN was detected in OV-90 cells (data not shown); therefore, lack of susceptibility of OV-90 cells to HCVpv infection might be attributable to lower expression of SR-B1 and hCD81 in OV-90 cells than in other cell lines (Fig. 1D and E). Thus, we selected JHH-4 and FU97 cells for further investigation of HCV propagation.

JHH-4 and FU97 cells permit HCV propagation. To examine the susceptibility of JHH-4 and FU97 cells to HCV propagation, HCVcc was inoculated into these cells at a multiplicity of infection (MOI) of 1, and intracellular HCV RNA and infectious titers in the culture supernatants were determined by qRT-PCR and focus-forming assay, respectively. FU97 cells exhibited higher levels of HCV gene expression than JHH-4 cells, and these levels increased continuously until 48 h postinfection; treatment with IFN-α significantly inhibited HCV gene expression in both JHH-4 and FU97 cells (Fig. 2A, left panels). In addition, substantial amounts of infectious particles were detected in the culture supernatants of JHH-4 and FU97 cells infected with HCVcc, in contrast to the lack of infectious particles in the culture supernatants of 293T-CLDN/miR-122 cells infected with HCVcc (Fig. 2A, bar graph). Recent reports have shown that exogenous expression of miR-122 enhances HCV RNA abundances in several hepatic or nonhepatic cell lines (16–18). Therefore, we examined the effect of miR-122 overexpression on HCV RNA abundances in both JHH-4 and FU97 cells. miR-122 was introduced in these cells by a lentiviral vector encoding pri-miR-122, an unprocessed miR-122, and miR-122 expression was confirmed by quantitative PCR (qPCR) analysis (Fig. 2B, bar graph). In contrast to the slight increase of HCV RNA in FU97 cells, JHH-4 cells exhibited a significant increase of HCV RNA, suggesting that the expression level of miR-122 is a key determinant for the efficient propagation of HCV (Fig. 2B, right panels). A previous study has shown that NS5A proteins were localized around the endoplasmic reticulum (ER) membrane, and accumulation of core protein around lipid droplets (LDs) facilitates efficient assembly of infectious particles in Huh7 cells (24). Immunofluorescence microscopy observation revealed that core and NS5A proteins in JHH-4 and FU97 cells infected with HCVcc were detected around LDs and in the ER together with double-stranded RNA (dsRNA), respectively (Fig. 2C). These results suggest that expression of liver-specific factors permits complete propagation of HCVcc in JHH-4 and FU97 cells and that hepatic characteristics play crucial roles in HCV propagation.

JHH-4 and FU97 cells permit complete propagation of HCVcc without any exogenous expression of host factors crucial for propagation of HCV. To further characterize the propagation of HCV in JHH-4 and FU97 cells, we examined the effects of the HCV inhibitors on the replication of HCV RNA. Preincubation with anti-HCV E2 antibody and pretreatment of cells with anti-hCD81 monoclonal antibody significantly inhibited HCVcc infection not only in Huh7 cells but also in JHH-4 and FU97 cells, suggesting that hCD81 is also involved in HCV entry into JHH-4 and FU97 cells (Fig. 3A, left panels). To examine the effect of miR-122 expression on HCV RNA abundances, cells were treated with LNA specific to either miR-122 (miR-122–LNA) or a non-specific LNA (Ctrl-LNA) at 6 h before infection with HCVcc. Treatment with miR-122–LNA but not with Ctrl-LNA significantly reduced the HCV RNA abundances in these cell lines, suggesting that miR-122 also plays a crucial role in the efficient propagation of HCVcc in JHH-4 and FU97 cells (Fig. 3A, right panels). Previous reports showed that treatment with MTTP inhibitors inhibited the production of infectious particles of HCVcc in Huh7 cells (20, 22). Although intracellular HCV RNA levels in Huh7, JHH-4, and FU97 cells were not inhibited by the treatment with MTTP inhibitors, including CP-346086 and BMS-200150 (Fig. 3B, left panels), the production of infectious particles was significantly decreased in these cells (Fig. 3B, right panels). These results suggest that the VLDL secretion pathway also participates in the propagation of HCV in JHH-4 and FU97 cells. Furthermore, it was shown that ApoB and ApoE are involved in the production of HCV particles in Huh7 cells (20–22). To confirm the role of ApoB and ApoE in HCV propagation in JHH-4 and FU97 cells, the expression of ApoB and ApoE was suppressed by siRNAs (Fig. 3C, left panels). The suppression of ApoB and ApoE expression significantly reduced HCV RNA levels in cells infected with HCVcc at an MOI of 1 (Fig. 3C, middle panels) and significantly reduced the infectious titers in the supernatants (Fig. 3C, right panels) at 72 h postinfection. Collectively, these results suggest that the JHH-4 and FU97 cells permit complete propagation of HCVcc without any exogenous expression of the host factors crucial for propagation of HCV, including receptor molecules, miR-122, and VLDL-associated proteins. FU97 cells exhibited higher susceptibility to HCVcc propagation than JHH-4 cells (Fig. 2A), and thus we characterized the FU97 cells in greater detail.

Establishment of HCV RNA replicon and cured cells by using FU97 cells. To further examine the characteristics of FU97 cells

Downloaded from http://jvi.asm.org/ on February 12, 2015 by OSAKA UNIV BIKEN MI

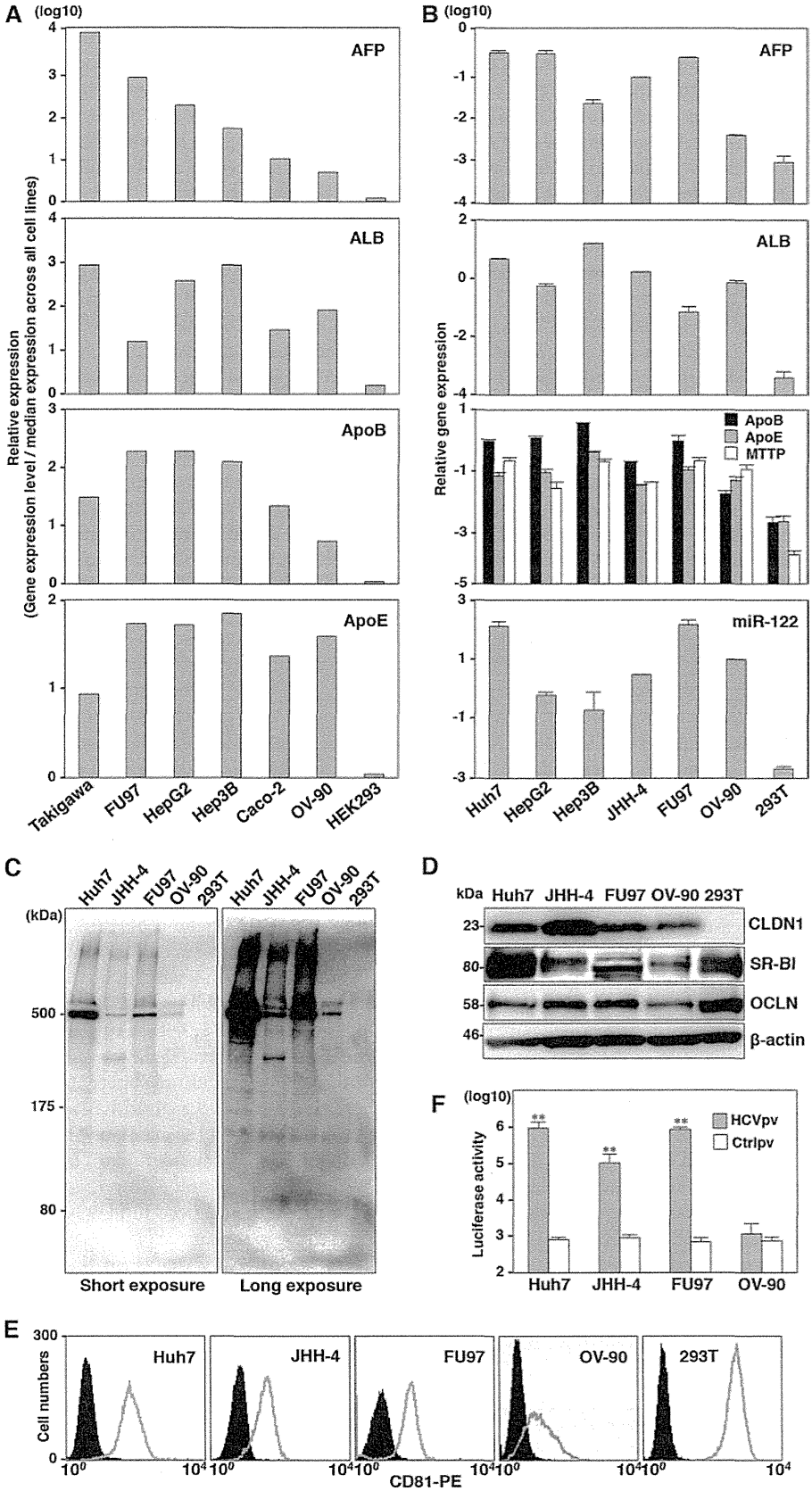

FIG 1 JHH-4 and FU97 cells express high levels of the liver-specific host factors required for HCV propagation. (A) Expression of AFP, ALB, ApoB, and ApoE in cancer cell lines screened by the NextBio Body Atlas application. The expression levels were standardized by the median expression across all cell lines. (B) Expression of AFP, ALB, ApoB, ApoE, MTTP, and miR-122 in AFP-expressing cell lines including HepG2, Hep3B, FU97, and OV-90 cells identified by NextBio

Downloaded from http://jvi.asm.org/ on February 12, 2015 by OSAKA UNIV BIKEN MI

with respect to HCV RNA replication, *in vitro*-transcribed subgenomic HCV RNA of the Con1 strain was electroporated into Huh7 and FU97 cells and cultured in medium containing G418 for a month, and then subgenomic replicon (SGR) cells of the Con1 strain were established (Fig. 4A). Replication of HCV RNA in four clones of the FU97 replicon cells was examined by qRT-PCR and immunoblotting. All clones contained a high level of HCV RNA (3×10^7 to 7×10^7 copies/μg total RNA) (Fig. 4B, upper panel), and the NS5A protein was also detected (Fig. 4B, lower panel). We examined the localization of NS5A and dsRNA in clone 5 of FU97 SGR cells by immunofluorescence analysis. Colocalization of NS5A with dsRNA was observed in clone 5, suggesting that the replication complex required for viral RNA replication was generated in the FU97 SGR cells (Fig. 4C). It has been shown that the infectivity of HCVcc in the cured cells that were established by elimination of the viral genome by treatment with antivirals from Huh7 replicon cells is significantly higher than that in parental Huh7 cells (49). To establish FU97 cured cells, two clones of FU97 replicon cells (clones 5 and 7) were treated with a combination of either 100 IU/ml of IFN-α and 100 nM BILN 2061 (clones 5-1 and 7-1) or 10 pM BMS-790052 and 100 nM BILN 2061 (clones 5-2 and 7-2) to eliminate viral RNA. Viral RNA was gradually decreased and was completely eliminated at 26 days posttreatment in four clones (Fig. 4D), and elimination of NS5A expression in cured cells was confirmed by immunoblot analysis (Fig. 4E). Next, to examine the susceptibility of the cured cells to the propagation of HCVcc, FU97 cured cell clones (clones 5-1 and 7-1) and parental FU97 cells were infected with HCVcc at an MOI of 1. The cured cells are more permissive to HCV infection, resulting in increased HCV RNA (Fig. 4F) and NS5A abundances (Fig. 4G) compared to the parental cells. These results suggest that susceptibility of the cured FU97 cells to the propagation of HCVcc is higher than that of parental cells, as seen in previous studies using hepatic and nonhepatic cells (17, 18, 49).

Cured FU97 cells exhibit normal innate immune response. It has been shown that one of the reasons for the high susceptibility of the cured cell line, Huh7.5 cells, to HCVcc infection is the impairment of the innate immune responses caused by mutation in RIG-I, a key sensor for viral RNA (50). To examine the involvement of the innate immune response in the enhancement of HCVcc propagation in the cured FU97 cells, the expression levels of IFN-stimulated gene 15 (ISG15) were determined upon stimulation with IFN-α or infection with VSV. Expression of ISG15 was significantly increased in both parental and cured FU97 cells by treatment with IFN-α or infection with VSV (Fig. 5A). To further confirm the innate immune responses in the cured FU97 cells, reporter plasmids encoding the luciferase gene under the control of either the IFN-β (Fig. 5B, left) or ISRE (Fig. 5B, right) promoter were transfected into both parental and cured FU97 cells and treated with IFN-α or inoculated with VSV. Activation of these promoters in the cured cells was comparable to that in the parental cells. To further assess the authenticity of viral RNA recognition and ISG induction pathways in the cured cells, nuclear localization of IRF3 and STAT2 upon stimulation was determined by immunofluorescence analysis. IRF3 and STAT2 in both parental and cured FU97 cells were translocated at similar levels into the nucleus upon infection with VSV or treatment with IFN-α (Fig. 5C). These results suggest that the efficient propagation of HCVcc in the FU97 cured cells is attributable to reasons other than impairment of innate immunity.

Expression of miR-122 is one of the determinants for HCV RNA abundances. We hypothesized that HCV replicon cells are capable of surviving in the presence of G418 by amplification of the viral genome through the enhancement of miR-122 expression, and cured FU97 cells acquired the ability to propagate HCVcc due to the high-level expression of miR-122. Our previous study also suggested that the expression levels of miR-122 in Huh7, Hep3B, and Hec1B cured cells were higher than those in parental cells (17, 18). To test this hypothesis, the expression levels of miR-122 in the cured FU97 cells were compared with those in parental cells. Interestingly, the cured FU97 cell clones exhibited a 1.8-fold increase in miR-122 expression (Fig. 6A). These results suggested that the efficient propagation of HCVcc in the cured FU97 cells was attributable to enhanced expression of miR-122 rather than the impairment of the innate immunity. To further confirm the correlation between the expression of miR-122 and HCV RNA abundances, we established FU97 cell lines expressing various concentrations of miR-122 by using a lentiviral vector (Fig. 6B), and HCV RNA abundances in these cell lines upon infection with HCVcc were determined by qRT-PCR (Fig. 6C). HCV RNA abundances increased in accord with the expression of miR-122, suggesting that expression of miR-122 is one of the determinants for HCV RNA abundances in cells infected with HCVcc.

HCV particles produced in FU97 cells exhibit similar characteristics to those in hepatic cells. To examine the characteristics of viral particles produced in FU97 cells, HCV particles recovered from the culture supernatants of Huh7.5.1 and FU97 cells infected with HCVcc were fractionated by buoyant density gradient analysis. Previous reports indicated that viral RNA and infectious particles were broadly distributed, with peaks in fractions from 1.13 to 1.14 g/ml and from 1.09 to 1.10 g/ml, respectively (51, 52). In agreement with the previous data, major peaks of HCV RNA and infectious particles in culture supernatants of both Huh7.5.1 and FU97 cells were detected around 1.10 g/ml and 1.09 g/ml, respectively (Fig. 7A and 7B, upper panels). Furthermore, ApoE was detected around the peak fractions of infectivity in both Huh7.5.1 and FU97 cells (Fig. 7A and B, lower panels). These results suggest that HCV particles produced in FU97 cells exhibit characteristics similar to those in hepatic cells.

Effects of anti-HCV drugs on the propagation of HCV in FU97 cells. To determine the difference in the efficacies of antivirals on the HCV propagated in Huh7 and FU97 cells, three DAAs, i.e., BMS-790052, PSI-7977, and BILN 2061 targeting NS5A,

Body Atlas and Huh7, JHH-4, and 293T cells was determined by qPCR. The relative expression of AFP, ApoB, ApoE, MTTP, and ALB mRNA was normalized to that of glyceraldehyde-3-phosphate dehydrogenase (GAPDH) mRNA, and that of miR-122 was normalized to that of U6 snRNA. (C) Secretion of ApoB in the culture supernatants of Huh7, JHH-4, FU97, OV-90, and 293T cells was determined by immunoblotting by using anti-ApoB antibody. The molecular mass of ApoB100 secreted from hepatocyte is about 500 kDa. (D) Expression of CLDN1, SR-BI, and OCLN in these cell lines was determined by immunoblotting. (E) Expression of hCD81 in the cell lines was determined by flow cytometry. (F) HCVpv-bearing HCV envelope proteins and control virus (Ctrlpv) were inoculated into the cell lines, and luciferase activities were determined at 24 h postinfection. Asterisks indicate significant differences (*, $P < 0.05$; **, $P < 0.01$) versus the results for control virus.

Downloaded from http://jvi.asm.org/ on February 12, 2015 by OSAKA UNIV BIKEN MI

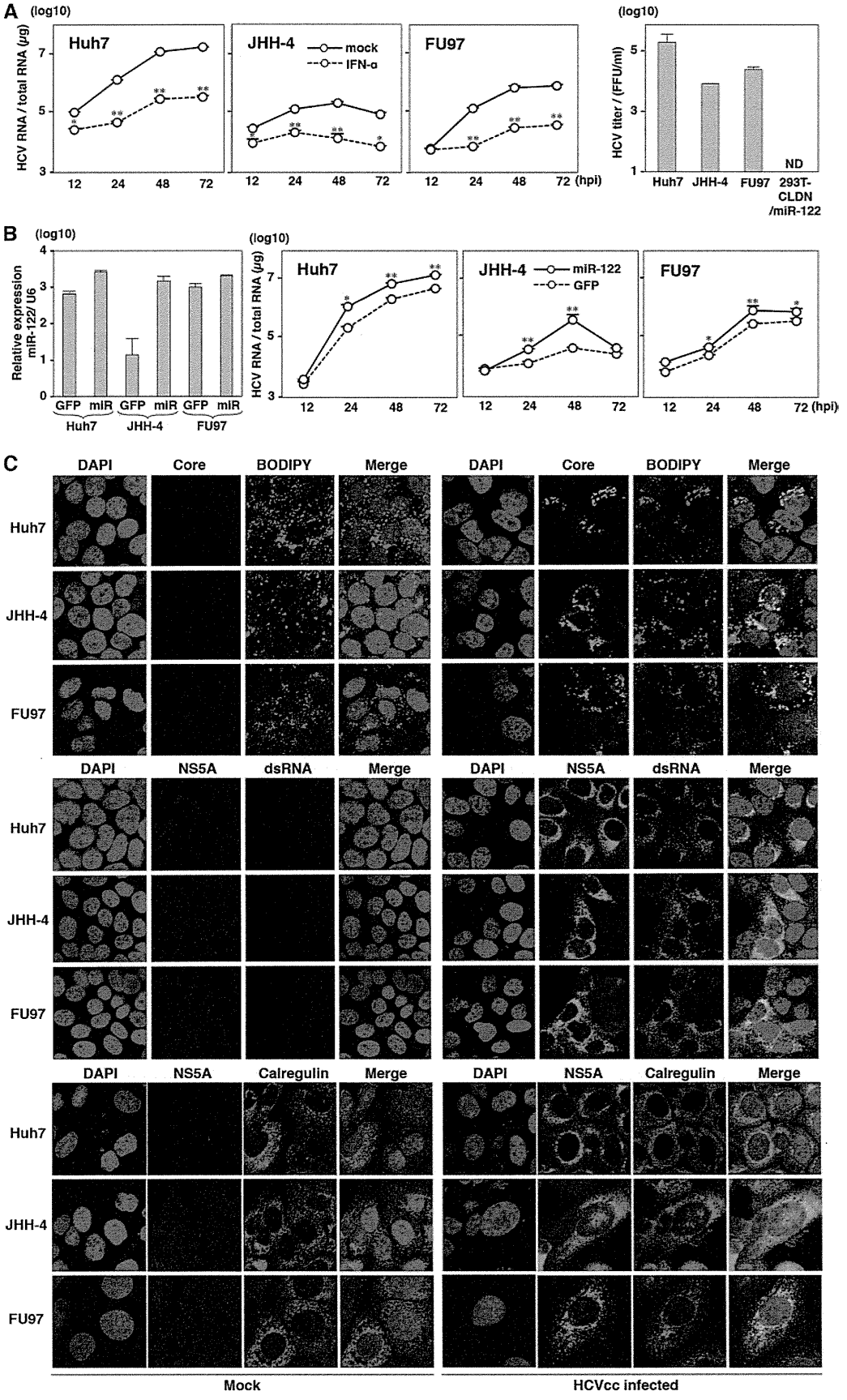

Downloaded from http://jvi.asm.org/ on February 12, 2015 by OSAKA UNIV BIKEN MI

NS5B, and NS3/4A, respectively, were treated with various concentrations at 3 h postinfection with HCVcc, and the intracellular HCV RNA level was determined by qRT-PCR at 48 h postinfection. Treatment with these DAAs inhibited the HCV RNA level in a dose-dependent manner in both Huh7 and FU97 cells (Fig. 8A, bar graphs) and exhibited no cell toxicity at all even at the highest dose (Fig. 8A, line graphs). The inhibitory effects of BMS-790052 (Fig. 8A, top graphs) on the propagation of HCVcc in FU97 cells were higher than those in Huh7 cells, and the 50% effective concentration (EC_{50}) values of BMS-790052 against propagation of HCVcc in FU97 and Huh7 cells were 7.2 and 21.8 pM, respectively ($P < 0.05$). On the other hand, the antiviral effects of BILN 2061 (Fig. 8A, bottom graphs) on the propagation of HCVcc in FU97 cells were lower than those in Huh7 cells, and EC_{50}s of BILN 2061 against propagation of HCVcc in FU97 and Huh7 cells were 65.0 and 38.9 nM, respectively ($P < 0.01$). PSI-7977 showed almost equivalent inhibitory effects to HCV propagated in FU97 and Huh7 cells, and the EC_{50}s of PSI-7977 against propagation of HCVcc in FU97 and Huh7 cells were 34.6 and 44.1 nM, respectively (Fig. 8A, middle graphs). These results suggest that the antiviral effect of DAAs on the propagation of HCVcc varied between Huh7 and FU97 cells.

Next, we examined the efficacy of IFN-α, RBV, and cyclosporine, which are inhibitors for HCV targeting host factors involved in the propagation of HCVcc (53–55), on the propagation of HCVcc in Huh7 and FU97 cells. Cells were treated with various concentrations of the reagents at 3 h postinfection with HCVcc, and the level of intracellular HCV RNA was determined by qRT-PCR at 48 h postinfection. In contrast to the treatment with DAAs, both Huh7 and FU97 cells exhibited cell toxicity by the treatment with RBV and cyclosporine but not with IFN-α at higher concentrations (Fig. 6B, line graphs). The inhibitory efficacies of IFN-α (Fig. 8B, top graphs) and cyclosporine (Fig. 8B, bottom graphs) on the propagation of HCVcc in FU97 cells were lower than those in Huh7 cells, and the EC_{50}s of IFN-α against propagation of HCVcc in FU97 and Huh7 cells were 4.3 and 2.5 IU/ml, ($P < 0.05$), respectively; those of cyclosporine were 6.9 and 3.2 μg/ml ($P < 0.01$), respectively. On the other hand, the antiviral effect of RBV on the propagation of HCVcc in FU97 cells was higher than that in Huh7 cells, and the EC_{50}s of RBV against propagation of HCVcc in FU97 and Huh7 cells were 99.0 and 198.9 μM, respectively ($P < 0.05$) (Fig. 8B, middle graphs). These results suggest that the efficacies of anti-HCV drugs targeting host factors involved in the infection of HCV were also different between Huh7 and FU97 cells.

FU97 cells exhibit higher susceptibility to HCVcc/JFH-2 propagation than Huh7 cells. HCVcc/JFH-2 was cloned from a patient with fulminant hepatitis and exhibited efficient propagation in Huh7 cured cells (34). *In vitro*-transcribed RNA of pJFH2/AS/mtT4 encoding a full-length JFH-2 strain was electroporated into Huh7.5.1 cells, and HCVcc/JFH-2 of 1.5×10^5 FFU/ml was recovered in the supernatants after serial passages. To examine the susceptibility of FU97 cells to the propagation of HCVcc/JFH-2, cells were infected with HCVcc/JFH-2 at an MOI of 1, and the intracellular HCV RNA level was determined by qRT-PCR. Intracellular HCV RNA in parental and cured FU97 cells increased until 72 h postinfection, while it reached a peak at 48 h postinfection in Huh7 cells, and the highest HCV RNA level was observed in the cured FU97 clones upon infection with HCVcc/JFH-2 (Fig. 9A). Infectious titers in the culture supernatants at 72 h postinfection with HCVcc/JFH-2 were also highest in the cured FU97 7-1 cells (2.5×10^4 FFU/ml), followed by parental FU97 (1.2×10^4 FFU/ml) and Huh7 (9×10^3 FFU/ml) cells (Fig. 9B). Next, we examined the expression and subcellular localization of HCV proteins in cells infected with HCVcc/JFH-2 by immunofluorescence analysis. Expression of NS5A in cells upon infection with HCVcc/JFH-2 was highest in the cured FU97 7-1 cells, followed by parental FU97 cells, and that in Huh7 cells was low (Fig. 9C, left panels). Core protein was detected around LDs in cells infected with HCVcc/JFH-2, as seen in those infected with the HCVcc/JFH-1 strain (Fig. 9C, right). To further confirm the efficient propagation of HCVcc/JFH-2 in FU97 cells, *in vitro*-transcribed viral RNAs of the JFH-1 and JFH-2 strains of HCVcc were electroporated into Huh7, FU97, and cured FU97 cells. Although the infectious titers of the JFH-1 strain in FU97 cells were lower than those in Huh7 cells, those of the JFH-2 strain in FU97 and cured FU97 cells were significantly higher than those in Huh7 cells (Fig. 9D). These results suggest that FU97 cells are more susceptible to propagate HCVcc/JFH-2 than Huh7 cells.

DISCUSSION

Several reports have shown that hepatic differentiation is involved in the susceptibility of ES/iPS cells to HCVcc infection (28, 30, 41). In addition, in hepatic cancer cell lines, including Huh7, HepG2, and Hep3B, cells derived from not poorly but well-differentiated HCC permit complete propagation of HCVcc (15–17), suggesting that hepatic differentiation is closely related to the susceptibility of cells to HCVcc propagation. In this study, we identified two cell lines susceptible to HCVcc infection by the screening of cancer cell lines expressing AFP as a marker of hepatic differentiation. HCC-derived JHH-4 cells and gastric cancer-derived FU97 cells permit complete propagation of HCVcc without any exogenous expression of the host factors required for HCVcc propagation, including HCV receptor candidates, miR-122, and apolipoproteins. In particular, FU97 cells exhibited higher susceptibility to HCVcc/JFH-2 infection than Huh7 cells, suggesting that FU97 cells would be useful tools for further HCV analyses.

Although HCV has been classified into seven major genotypes and a series of subtypes (56, 57), the *in vitro* infection model had been restricted to the JFH-1 strain based on the genotype 2a until

FIG 2 JHH-4 and FU97 cells permit HCV propagation. (A) Intracellular HCV RNA levels in Huh7, JHH-4, and FU97 cells inoculated with HCVcc at an MOI of 1, treated with 100 IU/ml of IFN-α or untreated (mock), were determined by qRT-PCR at 12, 24, 48, and 72 h postinfection (hpi). Infectious titers in the culture supernatants of Huh7, JHH-4, FU97, and 293T-CLDN/miR-122 cells infected with HCVcc at an MOI of 1 were determined by a focus-forming assay at 72 h postinfection (bar graph). (B) Exogenous expression of miR-122 in Huh7, JHH-4, and FU97 cells by lentiviral vector (bar graph). Total cellular miRNA extracted from the cells was subjected to qRT-PCR. U6 was used as an internal control. Intracellular HCV RNA in Huh7, JHH-4, and FU97 cells inoculated with HCVcc at an MOI of 1 was determined by qRT-PCR at 12, 24, 48, and 72 h postinfection. Solid and broken lines indicate HCV RNA abundances in miR-122-expressing and GFP-expressing control cells, respectively. (C) Huh7, JHH-4, and FU97 cells were infected with HCVcc at an MOI of 1, fixed with 4% PFA, and subjected to immunofluorescence analyses by using antibodies against core, NS5A, dsRNA, and calregulin. Lipid droplets and cell nuclei were stained by BODIPY and DAPI, respectively. Asterisks indicate significant differences (*, $P < 0.05$; **, $P < 0.01$) versus the results for control cells.

Downloaded from http://jvi.asm.org/ on February 12, 2015 by OSAKA UNIV BIKEN MI

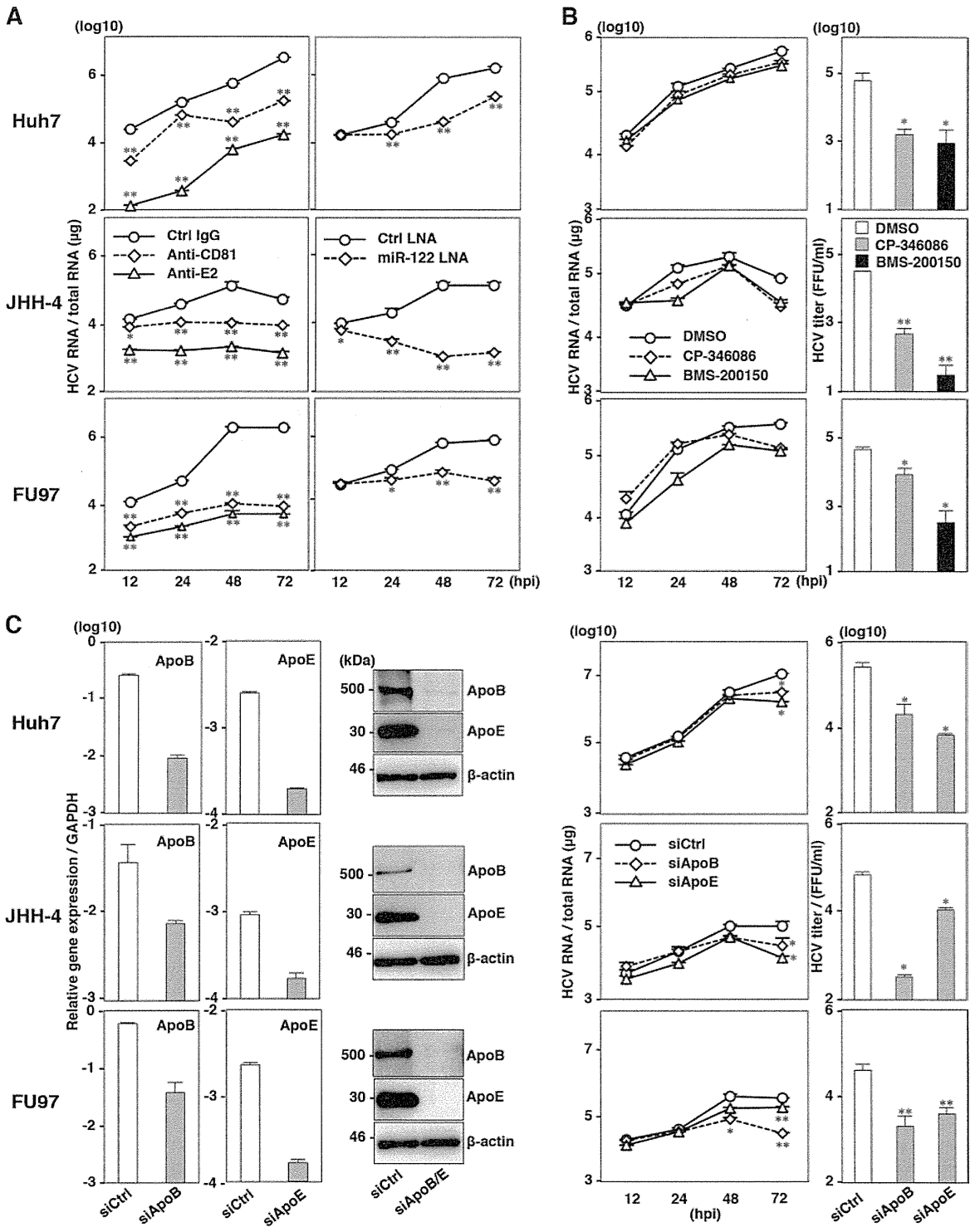

FIG 3 JHH-4 and FU97 cells permit complete propagation of HCVcc without any exogenous expression of host factors crucial for propagation of HCVcc. (A) Effect of inhibitors on the propagation of HCVcc in Huh7, JHH-4, and FU97 cells. (Left panels) HCVcc was preincubated with anti-E2 antibody and inoculated into cells. Cells were preincubated with anti-hCD81 antibody or isotype control antibody (Ctrl IgG) and then infected with HCVcc. (Right panels) Cells were infected with HCVcc and treated with miR-122-LNA (30 nM) or Ctrl-LNA (30 nM) at 6 h postinfection. (B) Huh7, JHH-4, and FU97 cells infected with HCVcc at an MOI of 1 were treated with dimethyl sulfoxide (DMSO) or MTTP inhibitor, CP-346086 (5 μM)or BMS-200150 (10 μM), at 3 h postinfection. Intracellular HCV RNA in cells at 12, 24, 48, and 72 h postinfection was determined by qRT-PCR (left panels). Infectious titers in the culture supernatants of cells infected with HCVcc at an MOI of 1 and treated with 5 μM CP-346086, 10 μM BMS-200150, or dimethyl sulfoxide alone (DMSO) at 3 h postinfection were determined at 72 h postinfection by a focus-forming assay (right graphs). (C) mRNA and protein expression levels of ApoB and ApoE (left panels) in Huh7, JHH-4, and FU97 cells at 48 h posttransfection with siRNA targeting either ApoB or ApoE or a control siRNA (siApoB, siApoE, or siCtrl, respectively) were determined by qRT-PCR and immunoblotting, respectively. Huh7, JHH-4, and FU97 cells were infected with HCVcc at an MOI of 1 at 6 h posttransfection with siRNA targeting either ApoB or ApoE or a control siRNA (siApoB, siApoE, or siCtrl, respectively) (right panels). Intracellular HCV RNA at 12, 24, 48, and 72 h postinfection and infectious titers in the culture supernatants at 72 h postinfection were determined by qRT-PCR and focus-forming assay, respectively. Asterisks indicate significant differences (*, $P < 0.05$; **, $P < 0.01$) versus the results for control cells.

Downloaded from http://jvi.asm.org/ on February 12, 2015 by OSAKA UNIV BIKEN MI

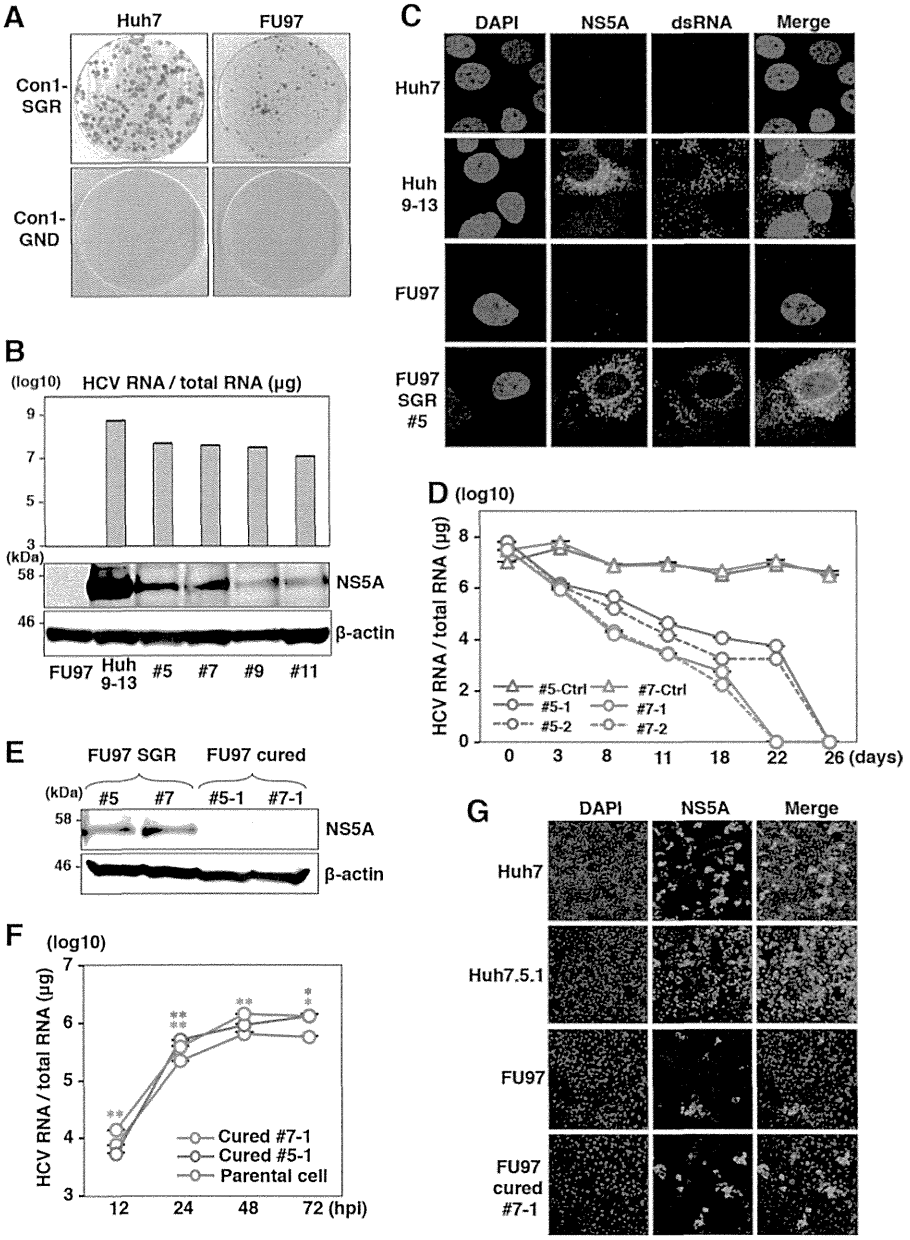

FIG 4 Establishment of HCV RNA replicon and cured FU97 cells. (A) Wild-type SGR RNA (Con1-SGR) or replication-defective RNA (Con1-GND) of the HCV Con1 strain was electroporated into Huh7 and FU97 cells and replaced with medium containing 1 mg/ml and 400 μg/ml of G418 at 24 h postelectroporation, respectively. Colonies were stained with crystal violet at 30 days postselection. (B) Four clones derived from FU97 SGR cells (clones 5, 7, 9, and 11) were subjected to qRT-PCR after extraction of total RNA (upper panel) and to immunoblotting using anti-NS5A antibody (lower panel). Huh9-13 cells, which were Huh7-derived Con1-SGR cells, were used as a positive control. (C) Huh9-13 cells, Huh7 parental cells, FU97-derived Con1-SGR cells (FU97 SGR, clone 5), and FU97 parental cells were fixed in 4% PFA and subjected to immunofluorescence assay using anti-NS5A and anti-dsRNA antibodies. Cell nuclei were stained by DAPI. (D) Elimination of HCV RNA from FU97-derived Con1-SGR cells. Two clones derived from FU97 SGR cells (clones 5 and 7) were treated with a combination of either 100 IU/ml of IFN-α and 100 nM BILN 2061 (clones 5-1 and 7-1) or 10 pM of BMS-790052 and 100 nM BILN 2061 (clones 5-2 and 7-2) to eliminate the HCV genome. Clones 5-Ctrl and 7-Ctrl are negative controls, untreated with anti-HCV drugs. Intracellular HCV RNA at 3, 8, 11, 18, 22, and 26 days posttreatment was determined by qRT-PCR. (E) The expression levels of NS5A in FU97 SGR cells (clones 5 and 7) and in FU97 cured cells (clones 5-1 and 7-1) were determined by immunoblot analysis using anti-NS5A antibody. (F) FU97 cured cells (clone 5-1 and clone 7-1) and parental cells were infected with HCVcc at an MOI of 1; the levels of intracellular HCV RNA at 12, 24, 48, and 72 h postinfection were determined by qRT-PCR. (G) The expression of NS5A in Huh7, Huh7.5.1, FU97, and cured FU97 clone 7-1 was determined by immunofluorescence analysis at 72 h postinfection by using anti-NS5A antibody. Asterisks indicate significant differences (*, $P < 0.05$; **, $P < 0.01$) versus the results for control cells.

recently (15). To clarify the pathogenesis of HCV depending on the genotypes, the establishment of cell-culture-adapted clones derived from various genotypes is essential (58). Viable JFH1-based intergenotypic recombinants, containing genotype-specific structural proteins, p7 and the complete or partial NS2, were generated for various genotypes of HCV (56, 59, 60). Although robust propagation systems of full-length HCV infectious clones of the H77 strain (genotype 1a) (61), TN strain (1a) (62), JFH-2 strain

Downloaded from http://jvi.asm.org/ on February 12, 2015 by OSAKA UNIV BIKEN MI